Assessing Spatial Variability in Swedish Ley Fields Through Field-Based Yield Estimates, Sentinel-2 Indices and Environmental Data

Wieland Schweizer

Master Thesis • 30 credits
Swedish University of Agricultural Sciences, SLU
Department of Crop Production Ecology
Environment Science (EnvEuro)
Uppsala, Sweden 2026

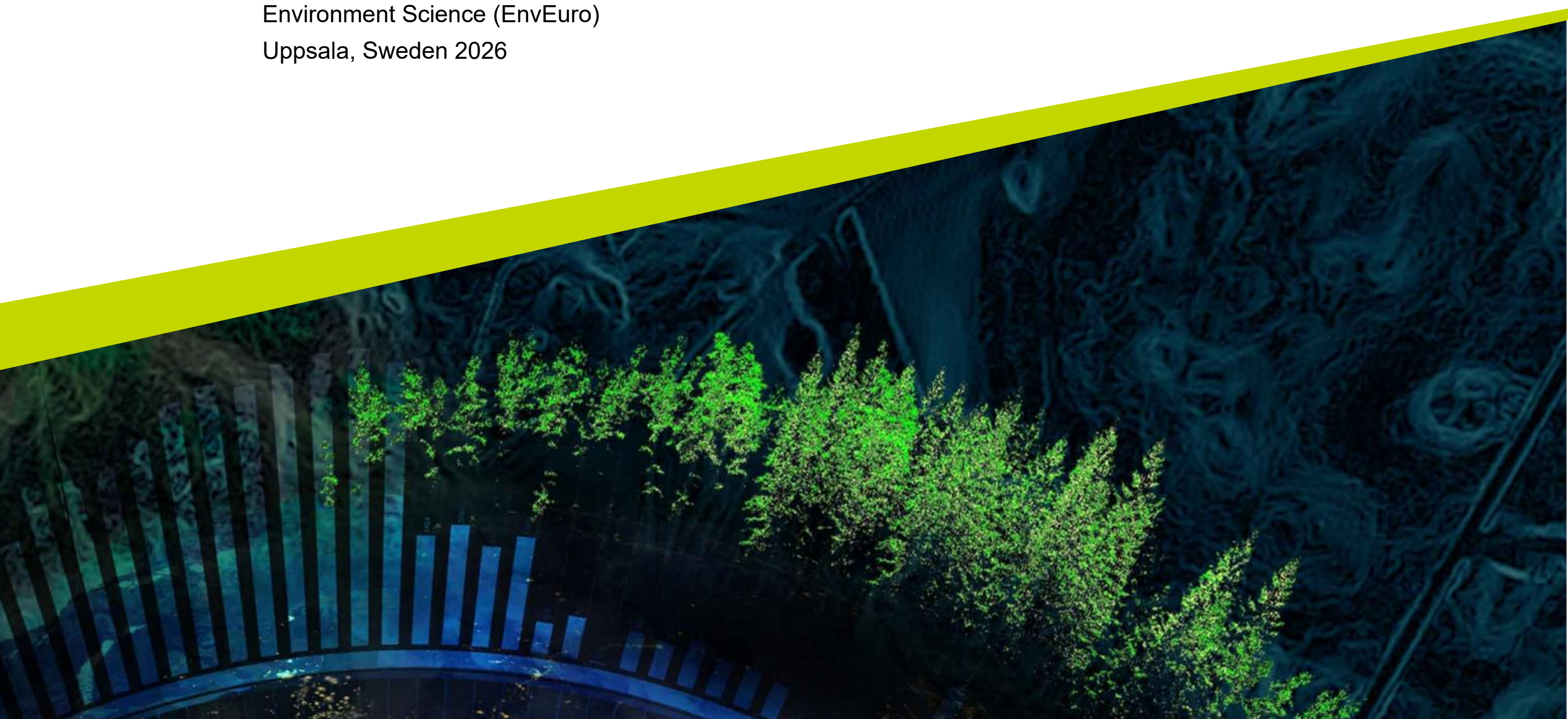

Assessing Spatial Variability in Swedish Ley Fields Through Field-Based Yield Estimates, Sentinel-2 Indices and Environmental Data

Wieland Schweizer

Supervisor:	**Julianne de Castro Oliveira, Swedish University of Agricultural Sciences, Department of Crop Production Ecology**
Assistant supervisor:	Emna Ayari, Swedish University of Agricultural Sciences, Department of Crop Production Ecology
Assistant supervisor:	Gernot Bodner, University of Natural Resources and Life Sciences, Vienna, Institute of Agronomy
Examiner:	Cecilia Palmborg, Swedish University of Agricultural Sciences, Department of Crop Production Ecology

Credits:	30
Level:	A2E
Course title:	Master thesis in Environmental Science
Course code:	EX0897
Programme/education:	Environmental Science (EnvEuro)
Course coordinating dept:	Department of Aquatic Science and Assessment
Place of publication:	Uppsala, Sweden
Year of publication:	2026
Copyright:	All featured images are used with permission from the copyright owner.
Keywords:	Temporary grassland, spatial yield variability, spectral vegetation index-based yield zones, Sentinel-2

Swedish University of Agricultural Sciences
Faculty of Natural Resources and Agricultural Sciences
Department of Crop Production Ecology

Abstract

Ley fields' dynamics can be spatially heterogeneous, and an understanding of within-field yield variability is important for improving fertiliser efficiency leading to sustainable forage production. This thesis assessed spatial variability in Swedish ley fields by comparing field-based dry matter yield estimates with Sentinel-2-derived yield-zone classifications, spectral indices, soil properties, meteorological data and topographic features. High- and low-yield zones had been pre-selected using multi-year Sentinel-2 Normalized Difference Vegetation Index (NDVI) medians. The results showed that the NDVI-based classification was mostly supported by estimated yield in ley fields. Most fields yielded higher than average yields in expected high-yield zones. However, the potential of this yield-classification varied between fields and was less effective in some cases. Other spectral indices showed plausible relationships with estimated yield depending on the farms' location and forage growth stages. Soil properties, topography and meteorological conditions provided useful field-specific context, but no single factor consistently explained the observed yield patterns across all sites. Overall, the study suggests that NDVI-based yield-zone classification can be a useful starting point for expected spatial productivity patterns in ley fields but should be combined with repeated field measurements and environmental data for more reliable interpretation. In addition, more advanced multivariate or machine-learning regression methods could be a better option for measuring within-field biomass variability.

Keywords: Temporary grassland, spatial yield variability, spectral vegetation index-based yield zones, Sentinel-2

Table of Contents

List of Tables

List of Figures

Abbreviations

Abbreviation	Description
NDVI	Normalized Difference Vegetation Index
EVI	Enhanced Vegetation Index
NDMI	Normalized Difference Moisture Index
NDWI	Normalized Difference Wetness Index
NDRE (B5)	Normalized Difference Red-Edge Index with the red edge band (S-2-B5, 705 nm)
NDRE (B7)	Normalized Difference Red-Edge Index with the red edge band (S-2-B7, 783 nm)
BSI	Bare Soil Index
TWI	Topographic Wetness Index
TPI	Topographic Position Index
DEM	Digital Elevation Model

1. Introduction

1.1 Scientific Context

Grasslands represent one of the most widespread terrestrial ecosystems, covering approximately one-third of the global land surface (excluding Antarctica) and playing a crucial role in supporting food production, biodiversity and key ecosystem processes (White et al. 2000; Suttie et al. 2005; Blair et al. 2014; Vitousek 2015). Beyond their ecological importance, grasslands are central to agricultural systems, particularly in livestock-based production systems, where they provide the primary source of forage. At the same time, grassland systems are subject to increasing pressures from land-use change, fragmentation, intensification, desertification, invasive species and climate change, which can inhibit their functioning, carbon storage potential and the ecosystem services they provide. Among the most important ecosystem services are erosion and flood control, carbon storage, biodiversity, water purification and recreation (Gibson 2009; Conant et al. 2017; Reinermann et al. 2020).

Within agricultural landscapes, grasslands can be broadly divided into permanent and temporary systems. Permanent grasslands are typically located in less favourable areas for agriculture, such as regions with, among other factors, challenging topography, soil conditions or climatic constraints and are often managed extensively. They are usually not part of a crop rotation and are maintained for more than five years (Milazzo et al. 2023). These systems are associated with high biodiversity and provide important ecosystem services, contributing to their high natural value (Peyraud & Peeters 2016).

Temporary grasslands, often referred to as ley fields, are sown with grass or grass-legume mixtures that are integrated into crop rotations for a limited period. Ley farming systems are widely used in temperate regions, including Northern Europe, where they contribute to forage production. Temporary grasslands can improve soil structure, enhance nutrient cycling and support soil organic matter accumulation (Hoeffner et al. 2021). In particular, the inclusion of legumes in ley mixtures can increase nitrogen availability through biological fixation, thereby reducing the need for mineral fertilisers and contributing to more sustainable production systems. In addition, legume-based systems seem to be better at storing soil organic carbon and produce less nitrous oxide (N_2O), a potent greenhouse gas (Drinkwater et al. 1998; Hayes et al. 2025).

Ley systems, like any field-based agricultural system, are not spatially uniform in their productivity or ecological functioning. Variability in soil properties such as texture, organic matter content, nutrient availability and pH can lead to substantial differences in biomass production within fields (Brady & Weil 2016). This spatial heterogeneity is particularly relevant for precision agriculture approaches where identifying high- and low-yielding zones can support more targeted management strategies (Robert 2002; Souza et al. 2025). Fertilisation is often applied uniformly, although soil properties, water availability and plant growth conditions vary considerably at small spatial scales (Robert 2002). In grassland systems, variable-rate nitrogen application has been investigated as an alternative to equal spatial distribution of fertiliser with the potential to reduce local nitrogen surplus or depletion within fields (Oenema et al. 2024). Improving the understanding of spatial yield variability is therefore essential for more efficient and sustainable grassland management.

To monitor grassland dynamics, destructive sampling of forage properties, particularly yield and quality, is limited in space and time. Remote sensing offers an alternative, providing high temporal and spatial resolution data covering a vast geographic area. By using spectral reflectance data from satellite sensors, vegetation properties can be assessed over large areas with a repeated spatial coverage at resolutions suitable for field- to landscape-scale analysis. This allows for cost-efficient, objective and reproducible data collection. Multispectral optical sensors (e.g. AVHRR, MODIS, Landsat, Sentinel-2) provide information on vegetation greenness, vitality and density, while hyperspectral sensors enable more detailed retrieval of biochemical and biophysical vegetation properties due to their higher spectral resolution compared to multispectral sensors. In addition, radar data acquired by sensors such as Sentinel-1 satellites, are sensitive to structural characteristics such as vegetation height, canopy structure and soil properties independent of cloud cover. Overall, remote sensing allows for large-scale analysis of both the quantity and quality of grasslands with high temporal and spatial resolution (Reinermann et al. 2020). It can be particularly valuable for detecting spatial and temporal variability in grassland systems, including changes driven by management and environmental factors However, remote sensing products often indirectly estimate biomass, and their interpretation can be influenced by various factors (Reinermann et al. 2020; Peng et al. 2023; 2024; Persson et al. 2024). Combined with field measurements and meteorological analyses, remote sensing methods can enable a more comprehensive understanding of yield variability within and between fields.

This thesis is implemented in a larger project dedicated to understanding yield variabilities in Swedish ley fields. The project is run under the name "*GödslingsOptimering i Vall: Detecting the causes of variability in ley fields to increase the efficiency of fertiliser management*" and comprises the collaboration between the Department of Crop Production Ecology at SLU, Lantmännen, Yara and DataVäxt. Several Swedish study sites have been chosen to be examined in regard to this topic.

1.2 Objectives

The objectives of this thesis were to analyse estimated yield variability as a function of soil properties, including textural and chemical composition, optical satellite-derived indices, meteorological data and Digital Elevation Model (DEM). This exploration aims to assess whether expected high- and low-yield zones exhibited different biophysical characteristics and whether these differences could be explained by any of the investigated factors.

This thesis is structured as follows: First, the theoretical background introduces the main concepts underlying yield variability, remote sensing indices, soil and topography influences and meteorological analysis. The Materials and Methods section then describes the study sites, field sampling design, laboratory analyses, satellite data processing, meteorological data and DEM-derived terrain variables. The Results section presents the estimated yields and evaluates differences between expected high- and low-yield zones using spectral indices, soil properties, topographic indices and meteorological conditions. Finally, in the discussion section, these findings are interpreted in relation to the classification of yield zones, the explanatory value of the different datasets and the limitations of the study.

1.3 Theoretical Background

Ley agriculture is a major sector in Sweden. Leys are commonly used for forage production and grazing and are often included in crop rotations with cereals and oil crops. They account for almost half of the country's cultivated agricultural area (Meurer et al. 2019). Ley seed mixtures are commonly used to increase yield stability, as different species vary in their strengths, limitations and responses to environmental conditions with timothy (*Phleum pratense L.*) and meadow fescue (*Festuca pratensis L.*) being the main grass species (Huss-Danell et al. 2007; Parsons et al. 2024). In Sweden, ley management usually involves three or more harvests per growing season, also in higher latitudes. Harvest strategies are complex and need to consider several factors, such as region of cultivation, plant species and plant maturity, as well as harvest timing and frequency. However, within a given site and growing season, earlier harvests, generally produce forage with higher crude protein concentration, lower fibre content and higher digestibility. Leys grown for forage production generally require fertilisation to maintain sufficient productivity. In Swedish ley systems, nitrogen, phosphorus and potassium are the main nutrients considered in fertilisation management. Nitrogen is particularly important for grass-dominated leys. Other nutrients, such as sulphur, magnesium and boron, may also be relevant depending on soil conditions, species composition and nutrient imbalances. Furthermore, the type of fertiliser can influence both nutrient availability and ley response (Parsons et al.

2024). Mineral fertilisers generally provide more directly plant-available nutrients in the short-term, whereas fertilisation with manure may maintain higher long-term levels of soil carbon, nitrogen and microbial activity in ley fields (Shi et al. 2022).

Under favourable growing conditions, such as under adequate nutrient and water availability, nitrogen can be taken up quickly by the crop. However, when ley-growth is limited, unused nitrogen may be lost to the environment (Van ’T Hull et al. 2025). Nitrogen losses from agriculture can have various negative impacts on human health and the environment, such as through eutrophication, ammonia emissions into the atmosphere or nitrate contamination in drinking water (Cameron et al. 2013; Johnson et al. 2024). Therefore, efficient fertilisation management is important to reduce nutrient losses and limit environmental and potential health impacts.

Spatial yield variability in ley fields results, among others, from interactions between plant growth, soil conditions, water availability, topography and weather. Differences in soil texture, organic matter, pH and nutrient availability can influence water retention, nutrient uptake and root development, thereby affecting biomass production (Brady & Weil 2016; Habib-ur-Rahman et al. 2022). At the same time, topographic variation and soil properties may govern local water distribution. Depressions may show higher soil moisture content, due to water accumulation from areas of higher elevation, and due to the accumulation of sediments from eroded soils from higher elevation, soil properties may be more beneficial for crop growth (Habib-ur-Rahman et al. 2022). Studies on corn and soybean, for example, have shown higher within-field biomass in topographic depressions due to favourable hydrological and soil-related conditions in these areas (Kravchenko & Bullock 2000; Beehler et al. 2017). However, while topography may contribute to within-field yield variability, its effect is strongly context dependent. Kravchenko et al. (2003), for example, found that other factors, such as precipitation or soil organic matter, can impact the effect of topography on yield variability.

To obtain and analyse topographic information, digital elevation models (DEMs) are commonly used. DEMs can be derived from different data sources, including light detection and ranging (LiDAR), aerial photogrammetry, stereo satellite imagery and radar-based methods such as interferometry. DEMs are usually a raster dataset, meaning it is made of pixels. A raster dataset contains a grid of pixels with each cell or pixel containing one or multiple values. In the case of a DEM, each pixel represents an elevation value, thereby creating a digital representation of the land surface topography (Florinsky 2016).

Satellite remote sensing uses sensors to measure electromagnetic radiation reflected from the Earth’s surface. In optical remote sensing, this mainly refers to reflected solar radiation in the visible, near-infrared and shortwave-infrared parts of the electromagnetic spectrum. These measurements are commonly expressed as surface reflectance. Since vegetation, soil, water and other land-cover types absorb and reflect radiation differently across the electromagnetic spectrum, satellite reflectance data can be used to assess surface properties (Horning 2019). The satellite images used in this thesis were obtained from the Sentinel-2 mission, launched by the European Space Agency in 2015. Sentinel-2 is an Earth observation mission consisting of polar-orbiting satellites. The mission was designed as a constellation of two satellites, phased at 180° to each other, providing a revisit time or temporal resolution of approximately five days at the equator. The Sentinel-2 satellites carry multispectral sensors, which record reflected radiation in 13 spectral bands from the visible to the shortwave-infrared region. These bands have different spatial resolutions, with four bands at 10 m, six bands at 20 m and three bands at 60 m spatial resolution (European Space Agency 2024). Spatial resolution describes the ground area represented by the smallest image unit, usually a pixel (Zhang & Li 2023). Smaller pixel sizes therefore correspond to higher spatial resolution and allow smaller-scale spatial variation to be captured. Each spectral band records reflectance within a specific wavelength range of the electromagnetic spectrum. Spectral resolution describes the ability of a sensor to distinguish between different wavelength regions and is determined by the number and width of its spectral bands (Pradham et al. 2008). Sensors with higher spectral resolution can capture more detailed differences in spectral information. In agricultural applications, this combination of repeated freely available observations, multiple spectral bands and relatively high spatial resolution makes Sentinel-2 satellites suitable for monitoring vegetation patterns and changes across fields and landscapes.

Remote sensing indices (i.e. mathematical combinations of reflectance values at different wavelengths) provide an indirect measure of vegetation properties because plant canopies interact with incoming radiation in characteristic ways. Healthy vegetation strongly absorbs red radiation through chlorophyll and reflects near-infrared radiation due to canopy structure, forming the basis for indices such as the Normalized Difference Vegetation Index (NDVI) and Enhanced Vegetation Index (EVI). Both regions, the near-infrared and red-spectral region, account for around 90% of vegetation information (Tucker 1979; Huete et al. 2002; Li et al. 2021). Red-edge indices, such as the Normalized Difference Red Edge index (NDRE), are more sensitive to chlorophyll-related variation and may remain informative under denser vegetation conditions (Gitelson et al. 2003; Delegido et al. 2011). Moisture-related indices such as the Normalized Difference Moisture Index (NDMI) use shortwave infrared reflectance, which is influenced by vegetation water content (Gao 1996). Soil-related indices such as the Bare Soil Index (BSI) are based on the contrast between the spectral reflectance characteristics of bare soil and vegetation. While vegetation strongly absorbs red radiation and reflects near-infrared radiation, bare soil exhibits relatively higher reflectance in the red and shortwave infrared regions (Mzid et al. 2021). Together, these indices can provide complementary information on vegetation biomass, chlorophyll status, bare soil presence and water-related stress.

2. Method and Materials

2.1 Study Sites

The study sites were selected across Sweden to diversify the climatic and farming practices variabilities from south to north: Varberg, Limmared, Tumba and Röbäcksdalen (RBD).
Figure 1 illustrates (a) the locations of study sites in Sweden together with the Köppen-Geiger climate classification and (b) field delineations with sampling points classified as expected high- or low-yield zones (further explanation can be found in the *Ground Truth Measurements* section).

Climate

According to the Köppen-Geiger climatic classification, illustrated in Figure 1, the selected farms in Limmared and Tumba are classified as having a warm-summer humid continental climate (Dfb), characterized by warm to hot summers and freezing winters. Precipitation can have drier and wetter periods but is usually distributed throughout the year. The Röbäcksdalen study site is located at the edge between warm-summer humid continental (Dfb) and subarctic climate (Dfc). A subarctic climate is characterized by short, cool summers and long, cold winters. Precipitation is spread through the year, generally scarce and mostly occurring during summer months. Finally, Varberg falls under the temperate oceanic climate (Cfb). This climate is characterized by warm summers, mild winters and a narrow annual temperature range. Frequent and moderate precipitation is common (Beck et al. 2023).

According to the Swedish Meteorological and Hydrological Institute (SMHI) report from 2024, the annual average temperatures for 1991-2020 for the weather stations closest to the study sites were: 8.3 °C (Varberg for Varberg), 6.8 °C (Ulricehamn for Limmared), 6.5 °C (Tullinge for Tumba) and 3.9 °C (Umeå Flygplats for Röbäcksdalen). The annual cumulative gauged precipitation for 1991-2020 was: 853.3 mm (Varberg for Varberg), 942.9 mm (Kindsboda for Limmared; 1993-2020), 575.6 mm (Tullinge for Tumba) and 634.7 mm (Röbäcksdalen for Röbäcksdalen). Due to inconsistencies in data availability across meteorological stations, the nearest available stations differed between temperature and precipitation datasets in some cases (SMHI 2024).

Management

Availability of management data was variable and partly incomplete across the study sites. For Varberg, records showed fertilisation with cattle manure and a nitrogen fertiliser NS 27-4 (27% nitrogen and circa 4% sulphur) in 2023, as well as at least two recorded harvests. In Limmared, field 23A was fertilised at least twice in 2023, whereas field 12B was fertilised at least once; no harvest records were available for these fields. In Röbäcksdalen, both fields were fertilised twice with YaraLiva Kalksalpeter (60% nitrogen, 0 % phosphorus and potassium) and twice with liquid manure in 2025. For Tumba, no management records were available.

Although the available management information was incomplete, the recorded fertilisation and harvest activities indicate that the studied ley fields were managed as production-oriented forage systems. Based on the available records and the general management context of the project, the fields were assumed to represent relatively intensively managed ley systems, characterised by fertilisation and multiple cuts per growing season.

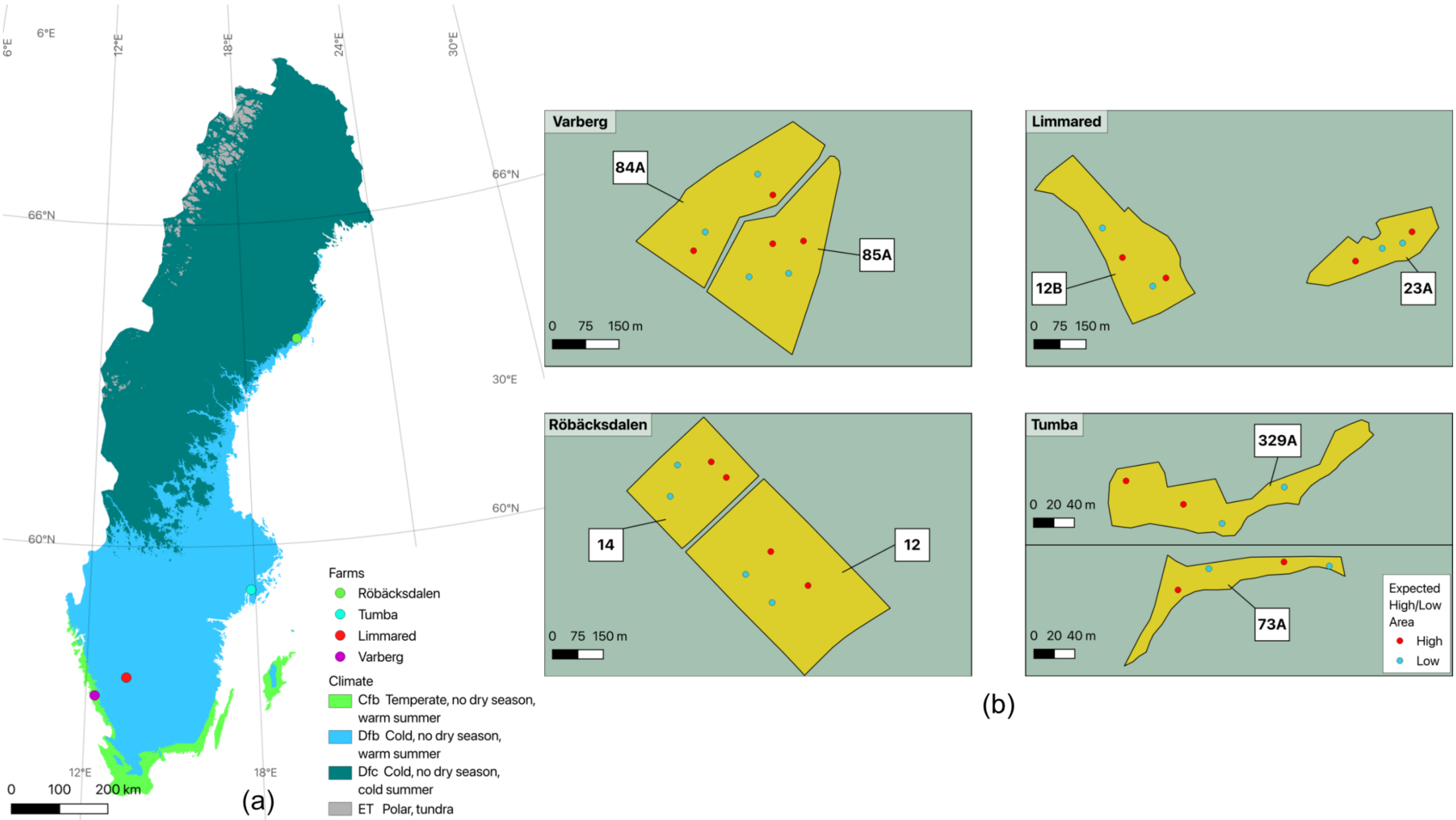

Figure 1: (a) Location of the selected study sites with Köppen-Geiger climate classifications (Beck et al. 2023). (b) Field delineations for selected study sites together with sampling points classified as expected high- or low-yield zone.

2.2 Data Collection

2.2.1 Ground Truth Measurements

The sampling was conducted prior to this thesis, and the author was not involved in the field sampling work. Sampling locations were pre-selected based on a time series of the Normalized Difference Vegetation Index (NDVI), derived from Sentinel-2 optical satellite data. Low- and high-yield areas were defined using median NDVI values calculated for the growing-season period from 15 May to the end of August in both 2023 and 2024.

For each farm, two fields were selected with four pixels of 10 x 10 m per field: two pixels with expected high yield (dark green circles in Figure 2) and two pixels with expected low yield (light green circles in Figure 2). This resulted in 8 sampling pixels per farm. Each sampling point corresponded to the centre of a Sentinel-2 pixel. The sampling occasions were planned to be just before the second harvest of the ley fields. In Röbäcksdalen, an additional sampling campaign was also performed before the third harvest. Field work was conducted around solar noon (± 2 hours) to ensure optimal illumination and consistency of measurements. In addition, field work was conducted shortly before the second

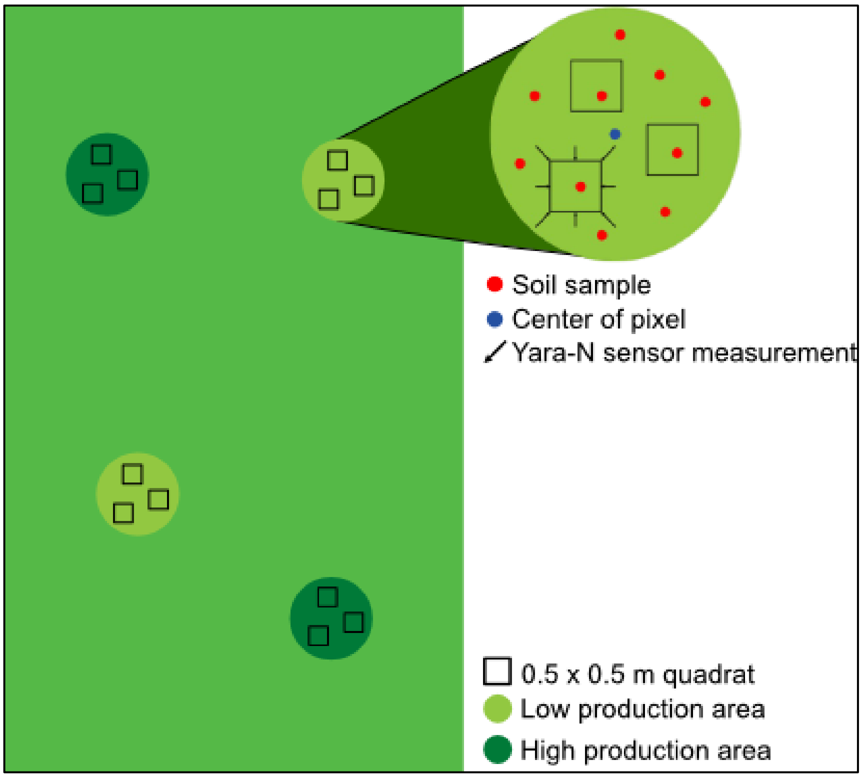

Figure 2: Sampling scheme developed for the sampling protocol. Two low-yield and two high-yield areas were selected per field. Within each area, ten soil samples were collected, along with vegetation samples from three quadrats per sampling area. Yara N-sensor measurements were taken from multiple angles around the quadrats (source: Gödslingsoptimering i Vall project).

harvest of the ley fields, apart from Röbäcksdalen where samples were also taken before the third harvest.

The centre of each pixel was marked using an RTK Emlid GPS sensor providing spatial positioning with centimetric accuracy. Within the pixel, three metallic quadrats of 50 x 50 cm were placed at less than 5 m radius of the centre (Figure 2). The botanical composition was visually estimated for the vegetation within each quadrat. Ley fields were dominated by grasses, which covered 60 - 97% of the quadrat surface, while white and red clover covered 1 - 40%.

For dry matter estimation, the vegetation within the quadrat was cut at approximately 8 cm height. The wet weight of the samples was measured. The samples were dried at 60°C for 48 hours. Dry weights were subsequently measured, and samples were sent to the laboratory for chemical plant composition analysis. Chemical plant composition was not considered for this thesis.

For soil analysis, for each pixel, a composite sample was collected in 10 different locations, dotted in red in Figure 2, at 20 cm depth. The combined samples were sent to a laboratory for standard chemical and textural analysis. Additionally, the Nitrogen content around the quadrats was quantified using Yara-N sensors. These measurements will not be considered for this thesis.

Yield Data

Yield data were computed from the weights of vegetation samples. For each pixel, the dry weights (DW, g) of the vegetation samples were averaged to obtain the average DW (g) per pixel, and this value was subsequently converted to an expected point-based yield (kg ha^{-1}). The yield (Y, kg ha^{-1}) was calculated according to the following equation:

$$Y = \frac{average\ DW}{1000 \cdot 0.25} \times 10\,000$$

This conversion accounted for the sampling area (0.25 m^2) and the transformation from grams to kilograms and from square metres to hectares. The range of yield values per farm was: Varberg before second harvest (2160 – 2880 kg ha^{-1}), Limmared before second harvest (1507 – 3227 kg ha^{-1}), Tumba before second harvest (1591 – 2616 kg ha^{-1}), Röbäcksdalen before second harvest (2368 – 3202 kg ha^{-1}) and Röbäcksdalen before third harvest (3418 – 4625 kg ha^{-1}).

Soil Properties

Soil samples collected at each pixel were analysed by a commercial laboratory. The following properties were determined: soil pH, plant-available phosphorus (P-AL, mg 100 g^{-1}), plant-available potassium (K-Al, mg 100 g^{-1}), plant-available magnesium (Mg-Al, mg 100 g^{-1}), calcium (Ca-Al, mg 100 g^{-1}), aluminium (Al-Al, mg 100 g^{-1}), iron (Fe-Al, mg 100 g^{-1}) and acid-extractable nutrients including potassium (K-HCl, mg 100 g^{-1}), phosphorus (P-HCl, mg 100 g^{-1}) and copper (Cu-HCl, mg kg^{-1}).

In addition, soil texture was assessed, including, clay, silt and sand content with humus (%).

2.2.2 Sentinel-2 Satellite Data

Satellite data used in this study were obtained from the European Space Agency Sentinel-2 mission. Sentinel-2 (S-2) satellites provide multispectral imagery with a spatial resolution of 10-60 m and a revisit time of approximately 5 days, covering a wavelength spectrum between 443 nm and 2202 nm. For this study, S-2 Level-2A surface reflectance data, processed using Google Earth Engine (GEE), were used, which had been atmospherically corrected. The use of GEE allows efficient satellite data filtering and spectral indices calculation without the requirement of image downloads, consequently, the requirement of data storage space. The S-2 collection "*Harmonized Sentinel-2 MSI: MultiSpectral Instrument, Level-2A (SR)*" was used (European Union/ESA/Copernicus 2021). The analysis focused on spectral bands in the visible, near-infrared (NIR), red-edge, and shortwave infrared (SWIR) regions, which are relevant for vegetation, soil and moisture indices. Specifically, bands B2 (blue, 493 nm), B3 (green, 560 nm), B4 (red, 665 nm), B5 and B7 (red-edge, 704 and 783 nm, respectively), B8 (NIR, 833 nm) and B11 (SWIR, 1614 nm) were utilised (European Space Agency 2024; 2025).

The used S-2 images were selected to be temporally as close as possible to the field sampling dates (see Table 1). Images were filtered by location, time and with the condition of cloudy pixel percentage < 20%. Finally, additional manual filtering of the images was done to avoid that less than 20% of cloudy pixels cover the study sites.

Table 1: Sampling and S-2 image acquisition dates, as well as the number of selected S-2 images per farm.

Farm Name	Sampling date (DD.MM.YY)	S-2 Image date (DD.MM.YY)	Number of selected S-2 images
Varberg	23.06.25	19.06.25	2
Limmared	12.06.25	20.05.25	3
Tumba	23.06.25	13.06.25	2
Röbäcksdalen (before 2nd harvest)	11.07.25	09.07.25	2
Röbäcksdalen (before 3rd harvest)	27.08.25	13.08.25	1

2.2.3 Meteorological Data

Meteorological data (temperature and precipitation) were obtained from the Swedish Meteorological and Hydrological Institute (SMHI 2025). The data provided were generated using the *Precipitation Temperature Hydrologiska Byråns Vattenmodell* (PTHBV; translated as *Hydrological Bureau Water Balance Model*) model, which was applied at a grid-scale of 4 x 4 km. A geostatistical interpolation method is used by SMHI to calculate grid data based on, among other factors, data from nearest weather stations. Further info about the interpolation techniques used can be found in Johansson (2000); Alexandersson (2003); Johansson & Chen (2003; 2005).

In this study, the temperature and precipitation data used were from 01 March to 31 October for the year 2025 and masked to the individual farms. Raster values were extracted for each farm polygon, considering only pixels intersecting the farm boundaries. For farms spanning multiple grid cells, values were averaged across the corresponding pixels.

2.3 Spectral Indices

Vegetation-related indices

Vegetation-related indices play a crucial role in understanding the composition and dynamics of vegetation. In this work, several indices were selected to better understand yield dynamics. One of the most widely used indices is the Normalized Difference Vegetation Index (NDVI) (Huete et al. 2002; Delegido et al. 2011). The NDVI was first proposed by Rouse et al. 1973:

$$NDVI = \frac{\rho_{NIR} - \rho_{red}}{\rho_{NIR} + \rho_{red}}$$

Where ρ_{NIR} and ρ_{red} correspond to spectral reflectance in the near-infrared (S-2-B8, 842 nm) and red (S-2-B4, 665 nm) bands, respectively.

NDVI is a simple and widely used index for estimating vegetation greenness and serves as an indicator of vegetation growth. However, NDVI is limited by its sensitivity to atmospheric conditions and soil background effects, as well as by influences from canopy structure. Additionally, it tends to saturate at high biomass levels and exhibits nonlinear behaviour (Van Der Meer et al. 2001; Huang et al. 2021; Huete et al. 2002). To alleviate some of the problems of NDVI, the Enhanced Vegetation Index (EVI) was chosen, which was first proposed by Huete et al. (2002):

$$EVI = G \cdot \frac{\rho_{NIR} - \rho_{red}}{\rho_{NIR} + C_1 \cdot \rho_{red} - C_2 \cdot \rho_{blue} + L}$$

Where $G = 2.5$ is the gain factor, $C_1 = 6$, $C_2 = 7.5$ are coefficients of the aerosol resistance term and $L = 1$ is the canopy background adjustment. ρ_{blue} corresponds to the reflectance in the blue band (S-2-B2, 490 nm). The reflectance values of the used S-2 images were scaled by a factor of 0.0001 to convert integer-based Sentinel-2 data to physically meaningful reflectance values (0-1). EVI is optimized to enhance the vegetation signals in high biomass regions while improving its sensitivity to atmospheric influences and canopy background effects (Vélez et al. 2023).

The Normalized Difference Red Edge index (NDRE) was used as a proxy for vegetation chlorophyll content:

$$NDRE = \frac{\rho_{NIR} - \rho_{RE}}{\rho_{NIR} + \rho_{RE}}$$

Where ρ_{NIR} and ρ_{RE} correspond to the near-infrared (S-2-B8A, 865 nm) and red edge bands reflectance (S-2-B5; NDRE (B5) or S-2-B7; NDRE (B7), corresponding to 705 and 783 nm, respectively). The red edge band information is highly sensitive to chlorophyll content in plants, even in dense vegetation. Therefore, NDRE is suitable for detection of subtle variations under dense vegetation cover (Gitelson et al. 2003; Vélez et al. 2023).

The Normalized Difference Moisture Index (NDMI) first proposed by Gao in 1996, is used as a proxy for vegetation water content. NDMI and the following NDWI are sometimes used interchangeably in the literature; for this thesis, indices were defined as follows.

$$NDMI = \frac{\rho_{NIR} - \rho_{SWIR}}{\rho_{NIR} + \rho_{SWIR}}$$

Where ρ_{NIR} and ρ_{SWIR} correspond to the reflectance in the near-infrared (S-2-B8, 842 nm) and shortwave infrared (S-2-B11, 1610 nm) bands. ρ_{SWIR} is strongly influenced by leaf water content due to high absorption of radiation by liquid water, while near-infrared reflectance (ρ_{NIR}) is primarily controlled by leaf structure (Gao 1996).

Open-water related indices

The Normalized Difference Water Index (NDWI) was first proposed by McFeeters in 1996, and used to detect open water features:

$$NDWI = \frac{\rho_{green} - \rho_{NIR}}{\rho_{green} + \rho_{NIR}}$$

Where ρ_{green} is the reflectance measurement in the green (S-2-B3, 560 nm) band. ρ_{NIR} corresponds to S-2-B8, 842 nm. The index takes advantage of the low reflectance in the NIR range and the high reflectance in the green band for water bodies (McFeeters 1996).

Soil-related indices

To separate bare soil from vegetation, the Bare Soil Index (BSI) was calculated using this equation:

$$BSI = \frac{(\rho_{SWIR} + \rho_{red}) - (\rho_{NIR} + \rho_{blue})}{(\rho_{SWIR} + \rho_{red}) + (\rho_{NIR} + \rho_{blue})}$$

Where ρ_{SWIR}, ρ_{NIR}, ρ_{red} and ρ_{blue} are the reflectance measurements in the shortwave infrared (S-2-B11, 1610 nm), near-infrared (S-2-B8, 842 nm), blue (S-2-B2, 490 nm) and red bands (S-2-B4, 665 nm), respectively (Mzid et al. 2021).

2.4 Digital Elevation Model (DEM)

Digital elevation data was obtained from Lantmäteriet, the Swedish governmental authority responsible for mapping, geospatial data and land registration. The spatial resolution of the downloaded terrain model ("*Markhöjdmodell*") was 1 x 1 m, above-ground objects such as vegetation and buildings had already been removed (Lantmäteriet 2026). Using the DEM, two topographical indices were computed: the Topographic Wetness Index and the Topographic Position Index.

Topographic Wetness Index (TWI)

The Topographic Wetness Index (TWI) was calculated using the SAGA (ver. 9.11.3) implementation in QGIS (ver. 3.44.9), which derives TWI from the local slope (β) in radians and the specific catchment area (SCA) according to the basic TWI formula:

$$TWI = \ln(\frac{SCA}{\tan\beta})$$

The index originates from TOPMODEL, a hydrological model, and expresses the tendency of a location to accumulate water as a function of upslope contributing area and slope gradient (Beven & Kirkby 1979). Higher TWI values indicate areas with greater potential for soil moisture accumulation, while lower values generally indicate drier, more draining locations. The use of DEM-derived terrain attributes for hydrological and environmental applications is further described by Moore et al. (1991), while the SAGA implementation follows methods described by Böhner & Selige (2006).

For the calculation of the Topographic Wetness Index (TWI), a 100 m buffer was first created around each field and applied to the digital elevation model (DEM) in order to reduce edge effects in subsequent flow accumulation analyses. To prepare the DEM for hydrologic analysis, surface depressions (sinks) were filled using the QGIS implementation of the Wang & Liu (2006) algorithm that can jointly determine flow paths and the spatial partition of watersheds.

Slope was derived from the processed DEM using the SAGA algorithm "*Slope, Aspect, Curvature*", applying the 9-parameter second-order polynomial method (Zevenbergen & Thorne 1987). The upslope contributing area (catchment area) was calculated using the SAGA "*Flow Accumulation (Top-Down)*" algorithm with the multiple flow direction method.

The resulting slope and specific catchment area layers were then combined to compute the Topographic Wetness Index using the SAGA "*Topographic Wetness Index (TWI)*" algorithm with default settings (i.e. no area conversion, no transmissivity variable and the TWI formula, as mentioned above, as method).

Topographic Position Index (TPI)

The Topographic Position Index (TPI) is a terrain-based metric that describes the relative elevation of a location compared to its surrounding neighbourhood. It is calculated as the difference between the elevation of a cell and the mean elevation of surrounding cells, allowing the identification of landscape positions such as ridges, slopes and valleys. Positive TPI values indicate locations that are higher than their surroundings, negative values indicate lower-lying positions and values close to zero indicate relatively flat areas (Weiss 2001).

For the calculation of the TPI, the DEM with the 100 m field buffer was used as input to the SAGA algorithm "*Topographic Position Index (TPI)*". In contrast to the TWI calculation, sink filling was not applied. The neighbourhood radius, also referred to as bandwidth in SAGA, was set to 50 m.

2.5 Data Processing and Statistical Analysis

Data processing and visualisation were mainly performed in RStudio (ver. 4.6.0) using R. For estimated yields, vegetation samples (see *Yield Data*) were averaged for each sampling location, resulting in 4 vegetation data points per field, 2 for each expected yield zone (high or low). Estimated yields were then calculated using the previously mentioned equation (see *Yield Data*) for each vegetation data point. Field estimated yields were calculated by averaging all 4 estimated yield data points. When distinguishing between high- and low-yield zones, averages were calculated for each of the 2 high- and low-yield zones per field. Farm-level yield estimates were calculated the same way, but by averaging all available vegetation sampling points within each farm rather than within individual fields.

The same approach of averaging between high- and low-yield sampling locations was used for the *Soil Analysis* section.

Field-level spectral index values were averaged over the whole field, considering all index values within a field. When low- and high-yield zones were considered, index values were averaged only for the corresponding sampling locations and the expected yield zone (high or low).

Within-field differences between high- and low-yield zones were calculated by subtracting the low zone average from the high zone average for both estimated yield and spectral index. Positive values therefore indicate higher values in the high-yield areas compared to the low-yield areas. On the other hand, negative values indicate higher values in the low-yield areas than in the high-yield areas. Values close to 0 indicate that differences between high (low) areas are minor.

Pearson correlation coefficients were calculated to assess linear relationships between estimated yield and spectral index values. Calculations were performed in Microsoft Excel (ver. 2604) using the PEARSON function. Correlations were calculated for the field averages (not considering yield zones) and, separately, for high- and low-yield zone averages. The Pearson correlation coefficient (r) was used to describe the strength and direction of the relationship. A correlation coefficient ranges from -1 to +1. Values between 0 and +1 indicate a positive correlation, with values closer to +1 indicating a stronger positive relationship. Values between -1 and 0 indicate a negative correlation, with values closer to -1 indicating a stronger negative relationship. Values close to 0 indicate little or no linear correlation. Furthermore, to assess statistical significance, the number of paired observations (n) was used to calculate the degrees of freedom as n - 2. The t-statistic was then derived using the equation:

$$t = \frac{r \cdot \sqrt{n-2}}{\sqrt{1-r^2}}$$

Finally, two-tailed p-values were calculated with the TDIST function using the t-statistic and the corresponding degrees of freedom. Correlations were considered statistically significant at $p < 0.05$.

3. Results

3.1 Estimated Yields

Figure 3 illustrates the estimated yield during the sampling year 2025 in the four selected farms: Limmared, Varberg, Röbäcksdalen (RBD) and Tumba. Points are coloured according to farm and shaped according to the expected yield zone (high and low) at the initial selection. Individual sampling points are visualised together with expected yield zone means. Error bars represent the standard deviation of samples around the mean. The highest yields were observed before the third harvest in RBD, exceeding 4000 kg ha $^{-1}$ in field 12. The lowest yields were observed in Limmared, field 23A, varying between 1507 and 2773 kg ha $^{-1}$.

The average yield per farm, regardless of yield zones, was lowest for Tumba (2040.67 kg ha^{-1}), followed by Limmared (2212.33 kg ha^{-1}), Varberg (2526.67 kg ha^{-1}), Röbäcksdalen before second harvest (2747.05 kg ha^{-1}) and Röbäcksdalen before third harvest (3922.35 kg ha^{-1}).

According to Figure 3, most of the expected high (low) yield zones, initially identified using Sentinel-2 images, are overlapping with high (low) yields in 2025.

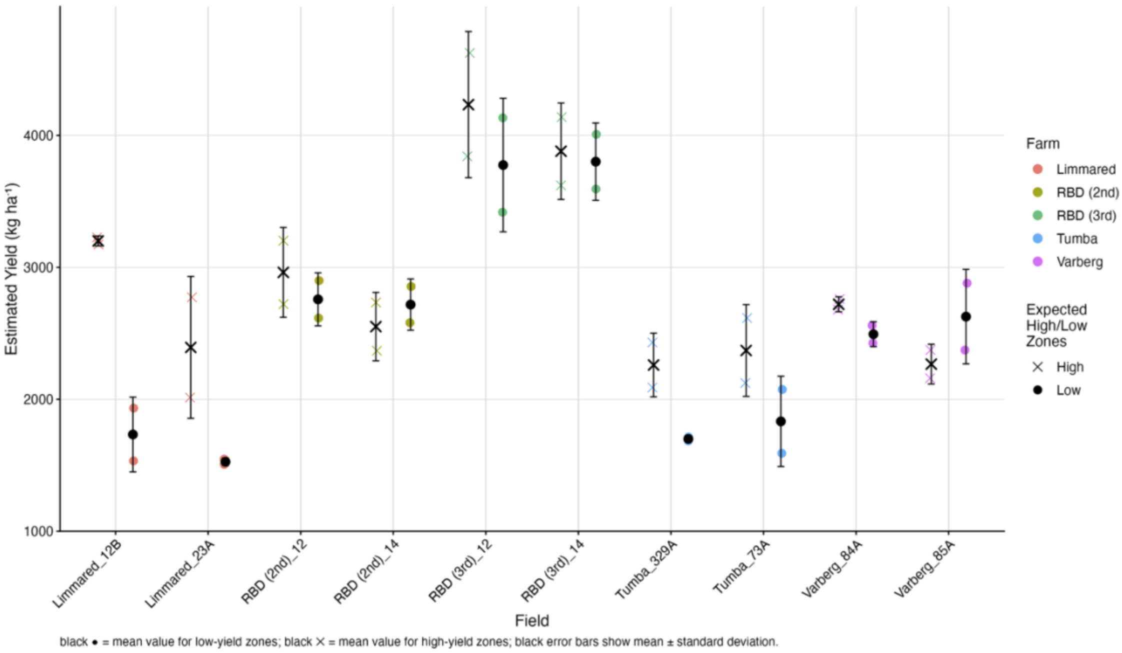

Figure 3: Scatterplot of estimated individual and average dry matter yields (kg ha^{-1}) by field and expected yield-zone. Coloured symbols represent individual samples and black symbols show zone-specific mean values; error bars indicate the standard deviation around the mean.

Notable exceptions were observed in Varberg 85A, where the expected low-yield zone exceeded the high-yield zone. A similar, though less pronounced, pattern was found in Röbäcksdalen 14 (before the second harvest).

Within-field yield variability between high and low zones differed substantially between sites. While some fields exhibited a strong yield difference between high- and low-yield zones, others showed only minor differences. This suggests that the classification of yield zones was more effective in some fields than in others.

The largest within-field yield difference between high- and low zones was recorded in Limmared 12B, where the high-yield zones exhibited an 84% higher average yield compared to the low-yield zones. The smallest within-field difference was recorded in Röbäcksdalen 14 (before the third harvest), where high yield-zone average yields were only 2% higher than the low yield-zone counterparts.

The largest yield variability in expected high-yield zones was observed in Röbäcksdalen 12 before the third harvest (3842 – 4625 kg ha^{-1}) and Limmared 23A (2013 – 2773 kg ha^{-1}). On the other hand, the smallest yield variability in these zones was observed in Limmared 12B (3174 – 3227 kg ha^{-1}) and Varberg 84A (2680 – 2760 kg ha^{-1}).

The largest yield variability in expected low-yield zones was observed in Röbäcksdalen 12 before the third harvest (3418 – 4133 kg ha^{-1}), Varberg 85A (2373 – 2880 kg ha^{-1}) and Tumba 73A (1591 – 2075 kg ha^{-1}). On the contrary, the smallest yield variability in the low-yield zone was found in Limmared 23A (1507 – 1547 kg ha^{-1}) and Tumba 329A (1685 – 1715 kg ha^{-1}).

3.2 Spectral Indices

A visual representation of the indices for one selected farm (Limmared), namely NDVI, EVI, NDRE (B5), NDRE (B7), NDWI, NDMI and BSI, can be seen in Figure 4.

In Figure 5, the calculated spectral indices, using Sentinel-2 data averaged per field, are illustrated. Pearson correlation analysis between mean estimated yield and mean spectral index values showed positive correlation coefficients (r) for NDVI, EVI, NDRE (B5) and NDMI. The strongest positive relationship was observed for NDMI ($r = 0.53$, $p = 0.24$), followed by NDVI ($r = 0.49$, $p = 0.15$) and EVI ($r = 0.41$, $p = 0.24$). NDRE (B5) showed the weakest positive relationship ($r = 0.18$, $p = 0.62$). On the other hand, NDRE (B7), NDWI and BSI showed negative correlations with increasing yields with BSI ($r = -0.52$, $p = 0.13$) and NDRE (B7) ($r = -0.50$, $p = 0.15$) displaying the strongest negative correlations, followed by NDWI ($r = -0.34$, $p = 0.34$). Farms with the lowest estimated yields (Limmared and Tumba) were characterized by the lowest index values for NDVI, EVI, NDRE (B5) and NDMI. The opposite is visible for indices NDRE (B7), NDWI and BSI. The difference in index values within a farm was most noticeable for Limmared for all indices. The smallest difference was seen in Röbäcksdalen (before third harvest) and Varberg, apart from higher differences for EVI, suggesting higher sensitivity for this index. Varberg achieved among the highest positive values for NDVI, EVI, NDRE (B5) and NDMI, while not having the highest estimated yield. Röbäcksdalen (before the third harvest), on the other hand, showed noticeably lower index values for the same indices while achieving the highest estimated yield values.

In Figure 6, the calculated spectral indices, averaged for each high (low) yield zone per field, were illustrated over the sampled farms. When distinguishing low- and high-yield zones (Figure 6), high-yield zones were not consistently associated with higher vegetation index values or with lower values in the case of NDRE (B7), NDWI and BSI. In the low-yield zones, Pearson correlation analysis showed the strongest and statistically significant correlation ($p < 0.05$) for NDVI ($r = 0.73$, $p = 0.02$). The weakest positive correlation was observed for NDRE (B5) ($r = 0.4$, $p = 0.25$). The strongest and weakest negative correlations were observed for BSI ($r = -0.52$, $p = 0.12$) and NDWI ($r = -0.46$, $p = 0.18$), respectively.

In the high-yield zones, NDMI ($r = 0.26$, $p = 0.46$) and EVI ($r = 0.16$, $p = 0.67$) marked the range for positive correlations, while BSI ($r = -0.25$, $p = 0.48$) and NDRE (B5) ($r = -0.01$, $p = 0.98$) set the range for negative correlations. Indices in low-yield zones generally showed stronger correlations to yields than high-yield zones. In some fields, such as Limmared 12B and Tumba 329A for EVI, differences between low- and high-yield zones were more clearly reflected in both index values and estimated yield. For some farms, such as Varberg or Röbäcksdalen (before third harvest), the index-yield-relation was generally much more clustered and the variability between high- and low-yield zones was minor.

To make assessing differences between expected high- and low-yield areas more approachable, a difference plot for indices and estimated yields per field was created in Figure 7. Field 329A in Tumba revealed to be a strong outlier for most of the indices, thus indicating that the difference between expected high- and low-areas is rather high compared to other fields. Furthermore, Limmared 12B represented a relatively high difference between indices and yields. NDRE (B7) generally showed a much more dispersed pattern and with that a much higher difference between the expected yield-zones than the other indices.

In summary, the indices most closely associated with estimated yield differed depending on the spatial grouping considered. At the field level, NDMI showed the strongest positive correlation with yield, followed by NDVI and EVI, while BSI and NDRE (B7) showed the strongest negative correlations. When considering high- and low-yield zones, NDVI showed the strongest and statistically significant positive relationship with yield in the low-yield zones. In contrast, high-yield zones showed generally weaker correlations. This suggests that NDMI and NDVI were the most informative positive vegetation indices for this analysis, whereas BSI and NDRE (B7) captured inverse relationships with yield. However, as most correlations were not statistically significant, these results should not be interpreted as definitive evidence of index performance.

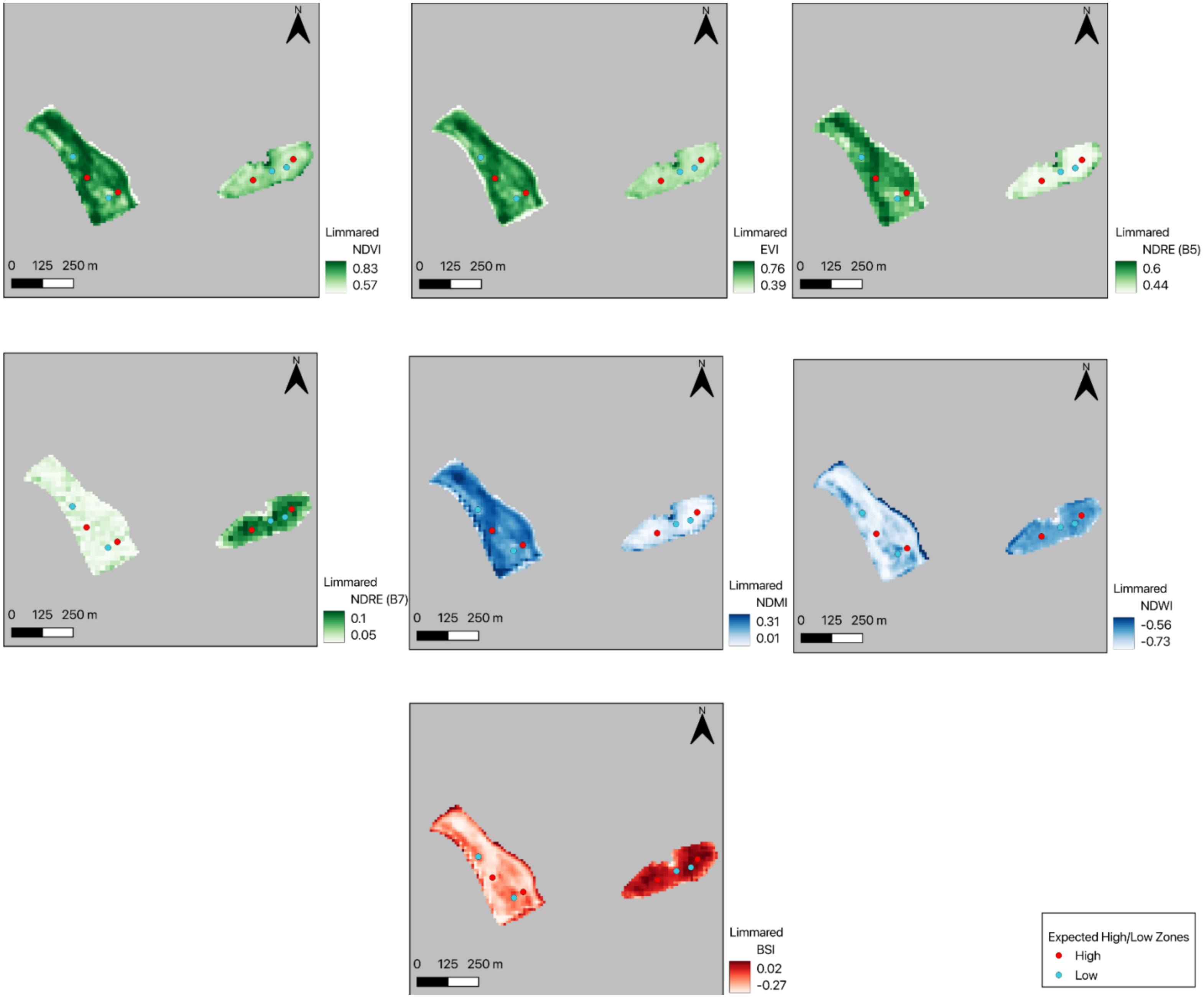

Figure 4: Visual representation of indices for Limmared 12B (left) and Limmared 23A (right). Red and blue points indicate expected high- and low- yield zones, respectively.

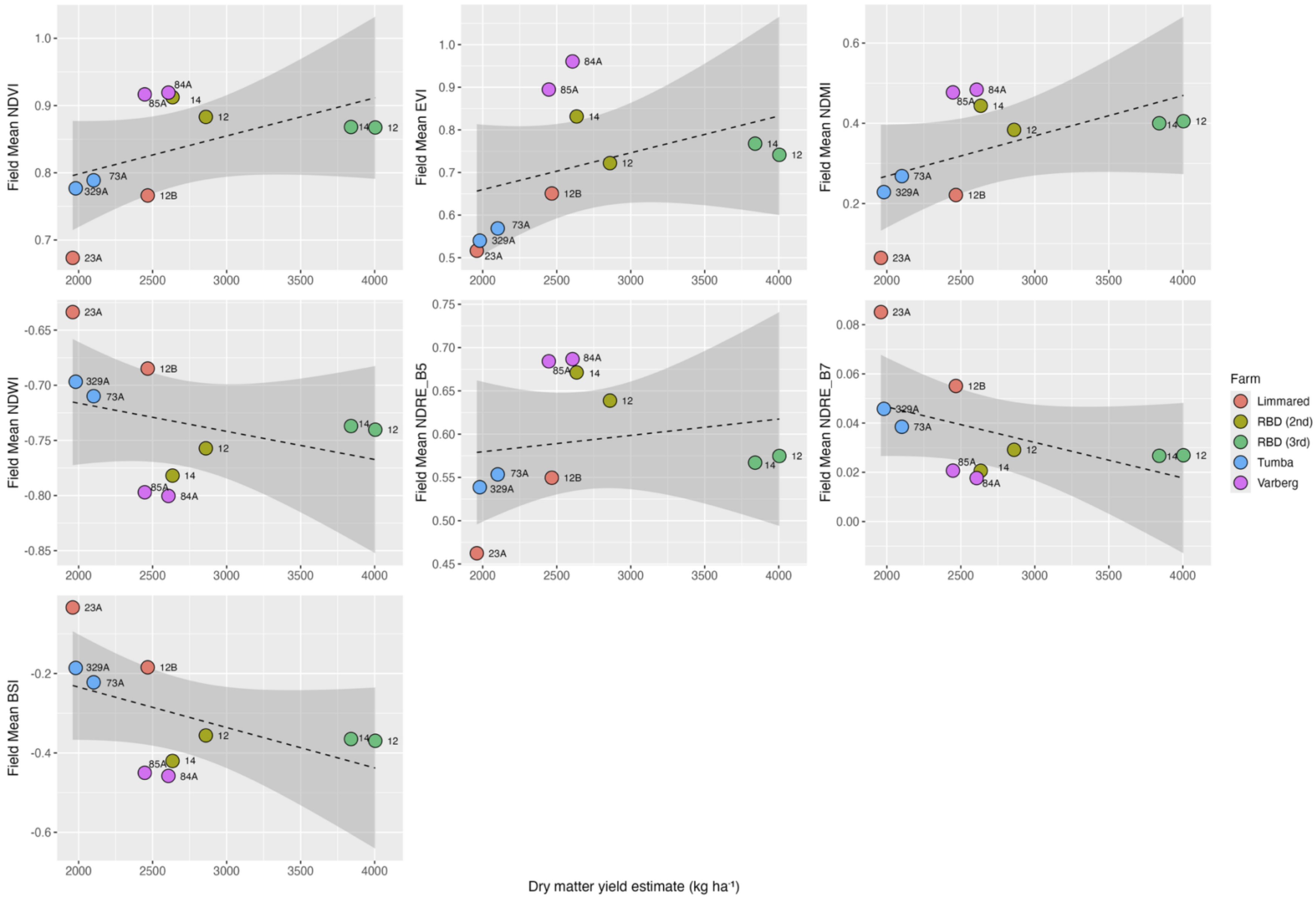

Figure 5: Scatterplots of the average values of spectral indices per field as a function of yields, coloured by farm.

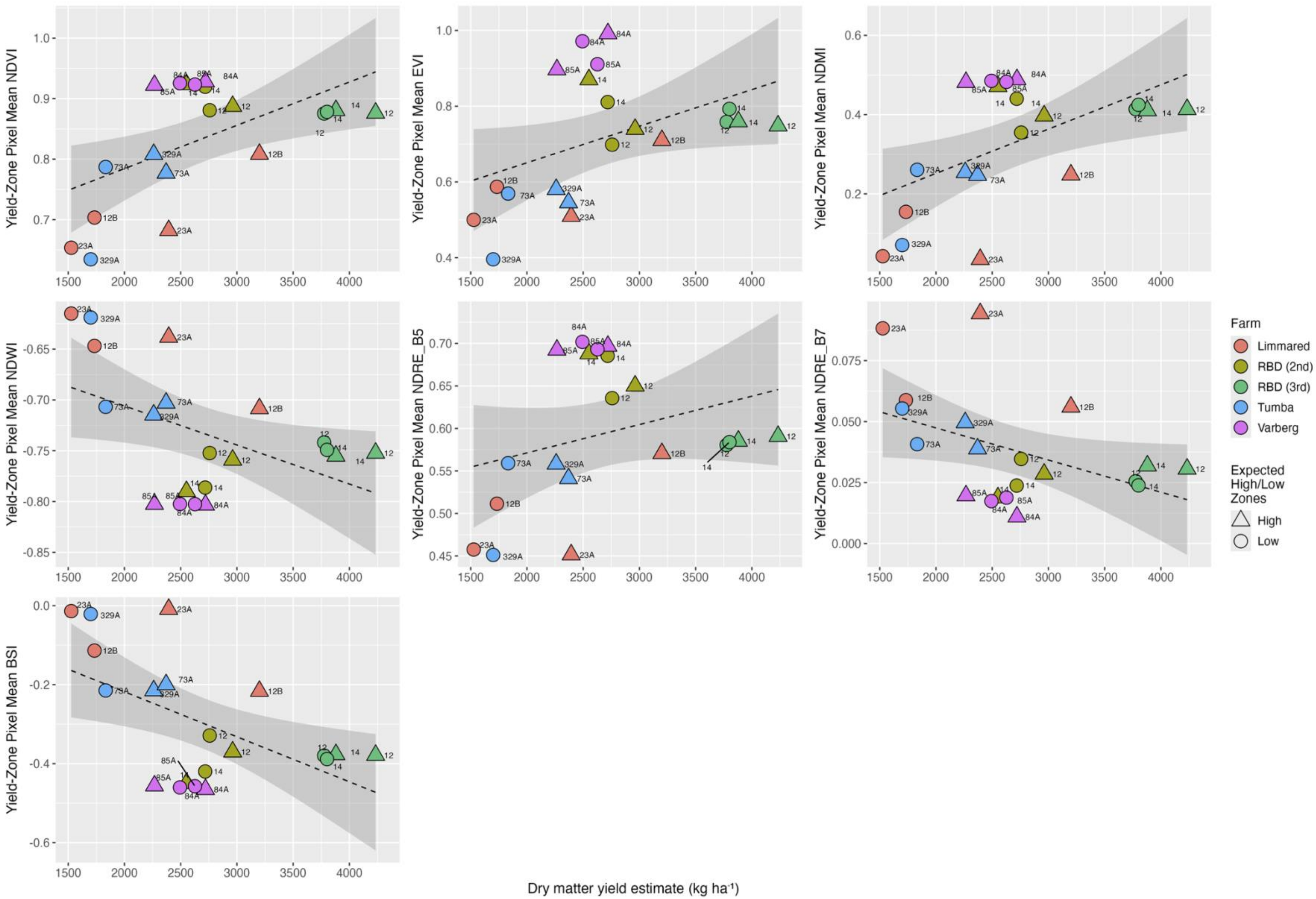

Figure 6: Scatterplots of the spectral indices averaged by field as a function of yields coloured by farm and shaped by expected yield (low or high).

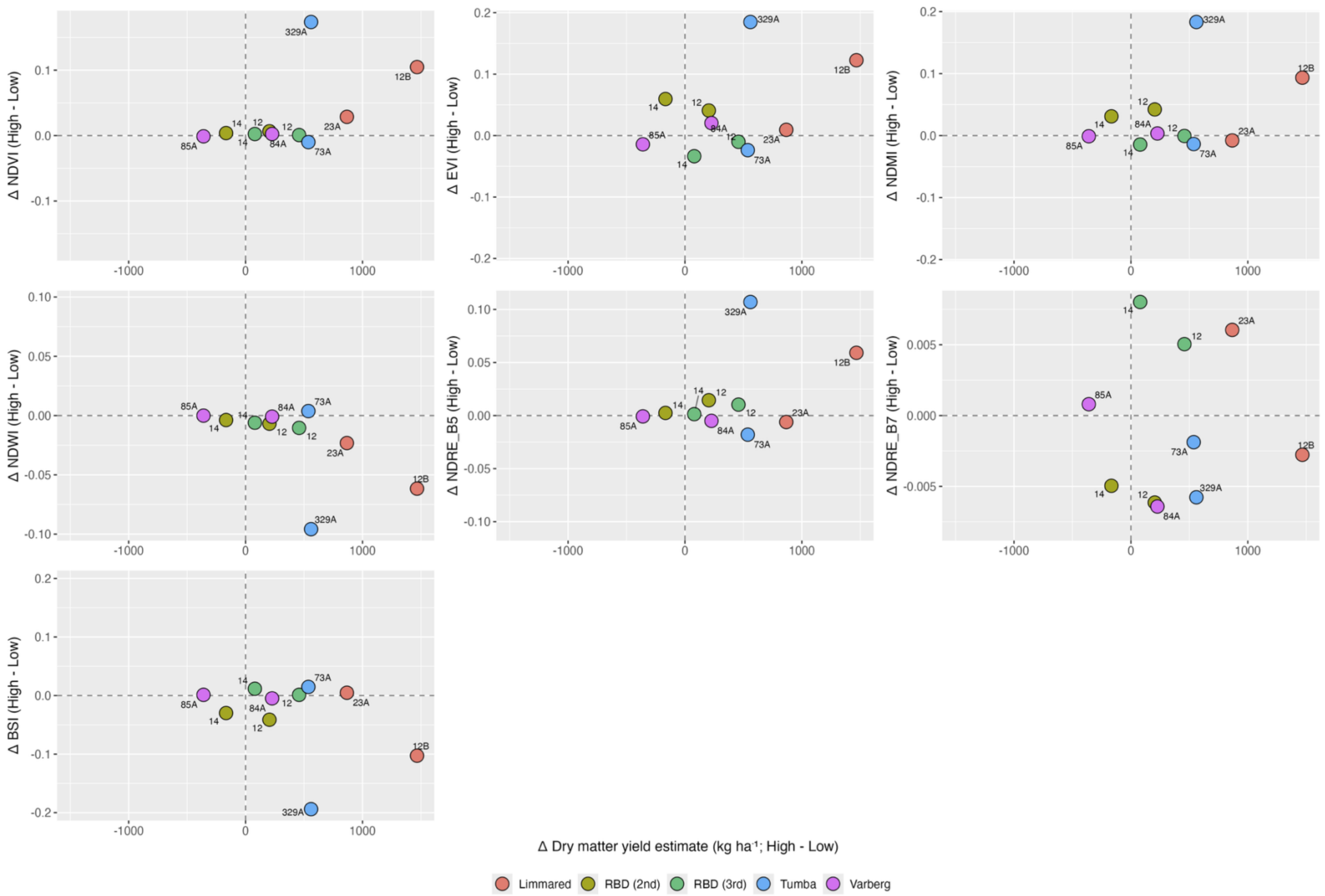

Figure 7: Scatterplots of differences between high- and low-yield areas per field for indices and estimated yields, coloured by farm.

3.3 Soil Analysis

3.3.1 Physical Properties & Humus

Figure 8 illustrates the distribution of soil texture (sand, silt and clay) and humus content for each sampled field and expected yield zone. Individual sample values are shown as coloured points, with colours indicating farms and point shapes distinguishing expected high- and low-yield zones. Black symbols indicate the mean value for each field and zone, while black error bars represent the variation around the mean using the standard deviation.

The average soil humus content across yield zones was generally below 10%, with the notable exception of field 12B in Limmared where the low-yield zones exhibited a substantially higher mean humus content of 35.5%. Regarding soil texture, the highest average silt contents were observed in Röbäcksdalen (68% for RBD before the second harvest and 71% for RBD before the third harvest), followed by Tumba (50%), Varberg (41%) and Tumba (24%). Silt content usually does not change over time, therefore Röbäcksdalen samples can be viewed as replicates. In contrast, the highest sand contents (60%) were recorded in Limmared, indicating a coarser soil texture in this area. Clay content was highest in Tumba (23%), with particularly high variability observed in the low-yield zones of field 73A (4-40%). Overall, low-yield zones exhibited greater variability

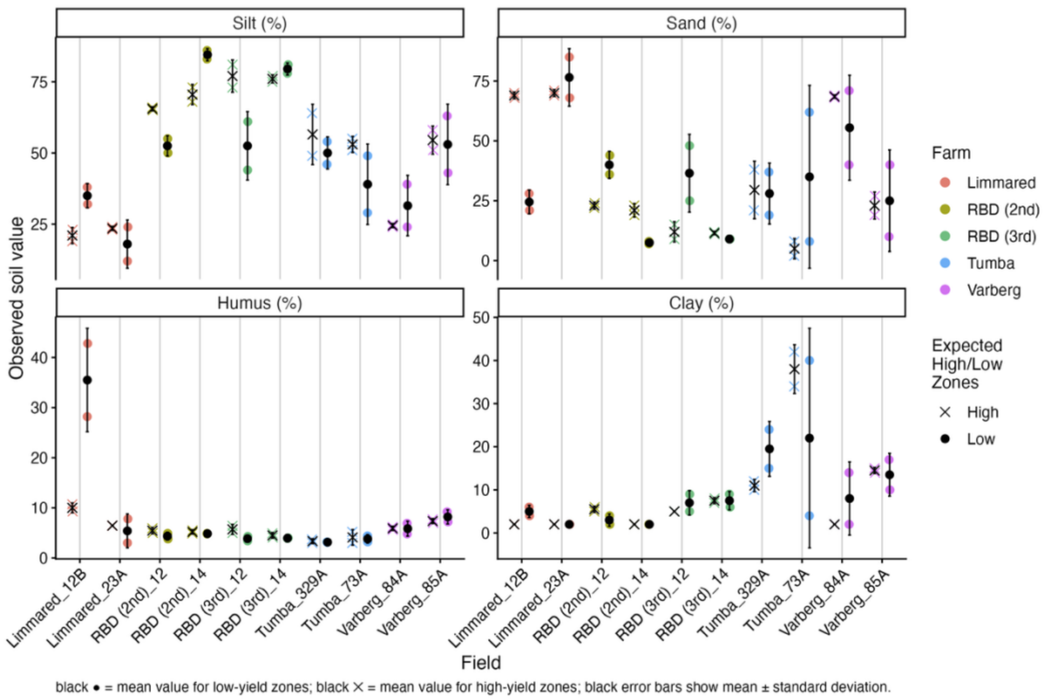

Figure 8: Scatterplots of individual soil sample values for soil physical properties and humus content by field and expected yield zone. Coloured symbols represent individual samples and black symbols show zone-specific mean values; error bars indicate the standard deviation around the mean.

in soil texture parameters compared to high-yield zones, suggesting more heterogeneous soil conditions in areas of expected reduced productivity.

3.3.2 Chemical Properties

Figure 9 illustrates soil chemical properties (pH, plant-available phosphorus (P-AL, mg 100 g^{-1}), plant-available potassium (K- AL, mg 100 g^{-1}), plant-available magnesium (Mg- AL, mg 100 g^{-1}), calcium (Ca- AL, mg 100 g^{-1}), aluminium (Al-AL, mg 100 g^{-1}), iron (Fe- AL, mg 100 g^{-1}) and acid-extractable nutrients including potassium (K-HCl, mg 100 g^{-1}), phosphorus (P-HCl, mg 100 g^{-1}) and copper (Cu-HCl, mg kg^{-1}) for each sampled field and expected yield zone. Individual sample values are shown as coloured points, with colours indicating farms and point shapes distinguishing expected high- and low-yield zones. Black

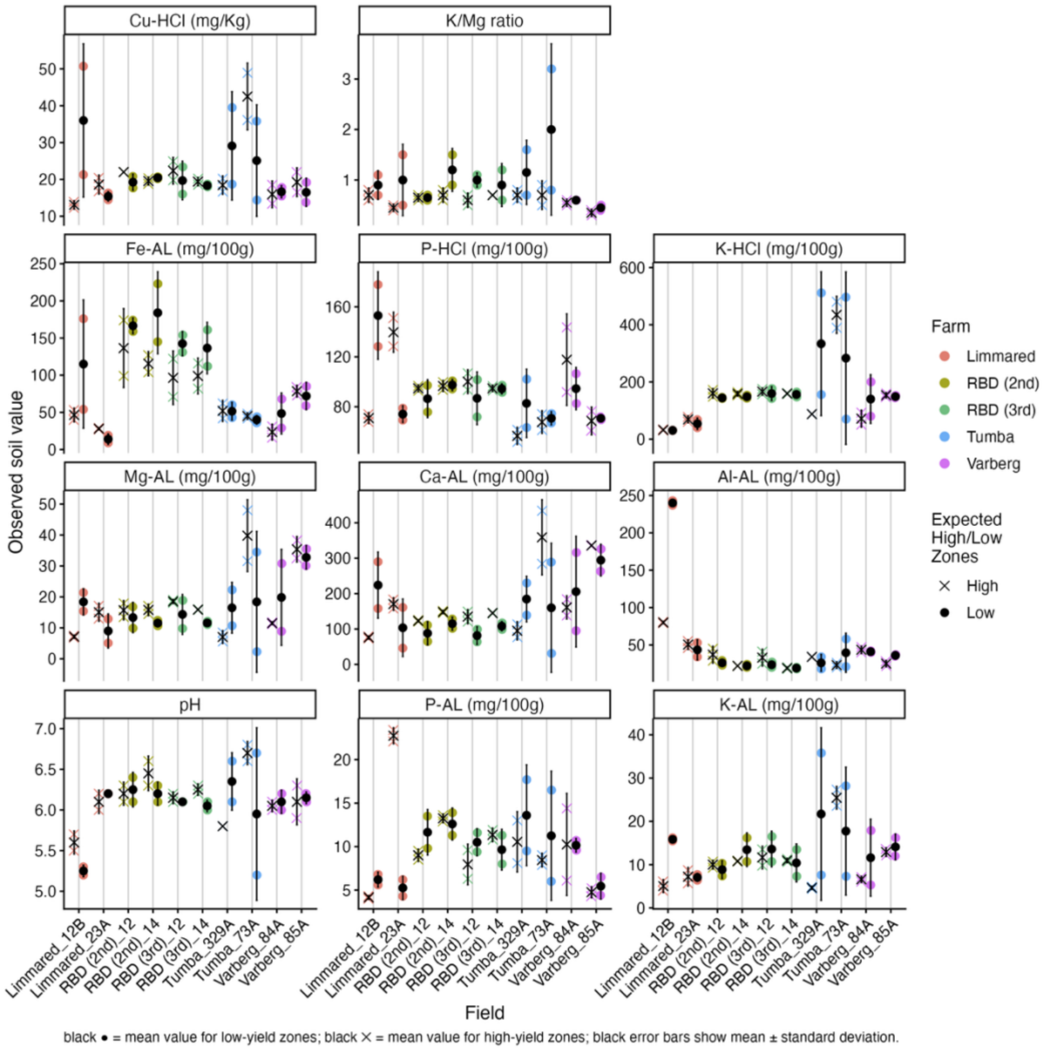

Figure 9: Scatterplots of individual soil sample values for soil chemical properties by field and expected yield zone. Coloured symbols represent individual samples and black symbols show zone-specific mean values; error bars indicate the standard deviation around the mean.

symbols indicate the mean value for each field and zone, while black error bars represent the variation around the mean using the standard deviation.

The average K/Mg ratio (absolute values ranging from 0.3 to 3.2) was generally higher in low-yield zones (0.96) compared to high-yield zones (0.61), indicating a relative imbalance between these nutrients under expected lower productivity conditions. The variability in the low-yield zones of Tumba 73A was high.

Cu-HCl levels were generally below 25 mg kg^{-1}, with higher average values mainly observed in the low-yield zones of Limmared 12B (36 mg kg^{-1}), Tumba 73A (25.1 mg kg^{-1}) and Tumba 329A (29.1 mg kg^{-1}). Tumba 73A was an exception, showing particularly high Cu-HCl (42.5 mg kg^{-1}) also in the high-yield zone. Variability was greatest in Limmared 12B and the Tumba fields.

Fe-AL levels were highest in the Röbäcksdalen fields compared to the other farms, with low-yield zones (172.25 mg 100 g^{-1}) generally showing higher average Fe-AL concentrations than high-yield zones (126 mg 100 g^{-1}). The lowest Fe-AL levels were recorded in Limmared 23A (17 mg 100 g^{-1}). Variability was highest in the low-yield zone of Limmared 12B.

Plant-available Phosphorus (P-AL) levels were highest in the high-yield zones of Limmared 23A (22.75 mg 100 g^{-1}). This stood out as the other Limmared fields showed comparatively low P-levels, as did Varberg 85A.

Average Aluminium (Al-AL) concentrations were elevated in Limmared (104 mg 100 g^{-1}), particularly in field 12B (160 mg 100 g^{-1}), whereas Al-levels in the other fields remained comparatively low, suggesting generally favourable conditions outside this site. In Limmared 12B, this pattern coincided with relatively low pH values (< 5.5), which may have contributed to increased aluminium availability.

The Tumba fields were characterised by a high degree of variability, especially within low-yield zones, which showed across multiple parameters (especially for pH, K-Al, Mg-Al, Cu-HCl, K-HCl). Overall, low-yield zones tended to show greater heterogeneity in soil chemical properties compared to high-yield zones. From the measured values, usually only K-AL and pH tend to change seasonally.

3.4 Meteorological Analysis

Meteorological data for 2025 from March to end of October were plotted in Figure 10. According to Figure 10, Varberg received the highest precipitation (669 mm), followed by Limmared (519 mm) and Röbäcksdalen (488 mm). Tumba received the lowest precipitation quantity of 395 mm. The wettest months were July, September and October for all farms. Temperature peaked in August, while precipitation was rather low for most farms during that time. Observed cumulative precipitation values for the same time interval in 2023 were: Varberg (908 mm), Limmared (869 mm), Tumba (476 mm) and Röbäcksdalen (450 mm). In 2024, observed precipitation sums were: Varberg (811 mm), Limmared (720 mm), Tumba (451 mm) and Röbäcksdalen (542 mm).

In the periods before sampling, Varberg and Limmared showed relatively high precipitation amounts (189 and 139 mm, respectively), while Tumba showed rather low precipitation (56 mm). On the other hand, Röbäcksdalen showed a rather balanced precipitation distribution before the sampling dates, with a relatively strong increase in precipitation between the two sampling dates (77 % increase). More specifically, most precipitation (91 mm) between the two sampling dates occurred over a period of two weeks at the end of July and the beginning of August. A second major precipitation event occurred in mid-August, when 22 mm of precipitation fell over a three-day period. The precipitation sums before sampling (starting in March) were: Varberg (189 mm), Limmared (139 mm), Tumba (56 mm), Röbäcksdalen before second harvest (156 mm) and Röbäcksdalen before third harvest (276 mm).

Mean daily temperature during the study period (March to end of October) was found to be highest in Varberg (12.5 °C), followed by Tumba (11.6 °C), Limmared (11.5 °C) and Röbäcksdalen (9.6 °C). Temperature-wise, Varberg, Limmared and Tumba proved to be similar to each other, while Röbäcksdalen showed a lower mean temperature. Observed mean daily temperature for the same time interval in 2023 were: Varberg (12 °C), Limmared (12.1 °C), Tumba (10.7 °C) and Röbäcksdalen (8.2 °C). In 2024, observed values were: Varberg (12.6 °C), Limmared (11.7 °C), Tumba (11.6 °C) and Röbäcksdalen (9.1 °C).

Regarding temperature, all farms showed a similar temperature pattern, except for generally lower temperature values for Röbäcksdalen. Between the first and second sampling dates for Röbäcksdalen, a temperature peak can be observed, followed by a sharp drop. The daily mean temperature values before sampling (starting in March) were: Varberg (9.7 °C), Limmared (8.2 °C), Tumba (8.4 °C), Röbäcksdalen before second harvest (6.6 °C) and Röbäcksdalen before third harvest (9.5 °C). Daily mean temperature between first (11.07.) and second (27.08.) sampling date at Röbäcksdalen was 17.5 °C.

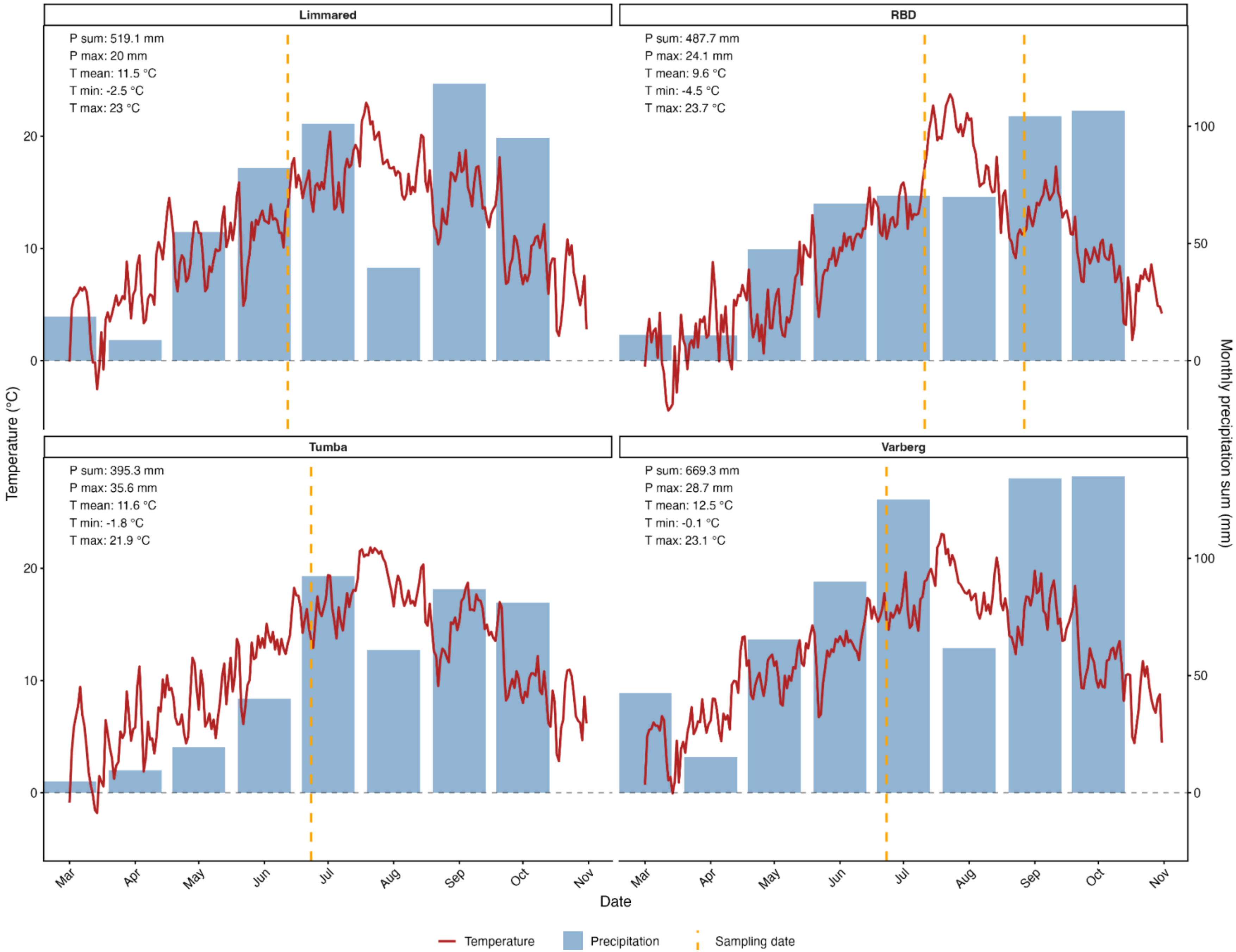

Figure 10: Subplot of monthly cumulative precipitation (histograms in blue), daily temperature (lines in red) and sampling dates, marked in orange, with the corresponding statistical metrics (minimum, maximum and average) for precipitation and temperature for the period March – November in 2025.

3.5 Topographic Wetness Index (TWI) & Topographic Position Index (TPI)

Figure 11 to Figure 13 illustrate the maps of the Topographic Wetness Index (TWI) and the Topographic Position Index (TPI) for the sampled farms.

According to Figure 11, both Varberg (fields 84A and 85A) and Röbäcksdalen (fields 12 and 14) TWI values highlighted areas of potential water accumulation with higher values generally occurring in lower-lying parts of the fields. In Röbäcksdalen, these wetter zones were more clearly structured along linear depressions, whereas in Varberg the pattern appeared more heterogeneous and less clearly defined. Röbäcksdalen showed a more pronounced micro-topographic structure with clearer ridges and furrows indicating drainage channels. On the other hand, Varberg shows a smoother topographic gradient with less distinct variation in field 85A. In field 84A, topography was shaped by a stronger elevation gradient. The distribution of expected high- and low-yield zones did not show a fully consistent relationship with either TWI or TPI. While some high-yield points were located in areas of intermediate moisture conditions, both high- and low-yield zones occurred across a range of TWI and TPI values. The within-field ranges of the digital elevation model were: Varberg (84A; 10.85 – 32.65 m), Varberg (85A; 6.21 – 12.39 m), Röbäcksdalen (12; 4.2 – 6.22 m) and Röbäcksdalen (14; 5.38 – 7.04 m).

In Limmared (Figure 12), fields were characterised by small elevation differences with only minor depressions and elevated areas. The within-field ranges of the DEM were 12B (160.52 – 165.81 m) and 23A (166.93 – 174.87 m). High- and low-yield points occurred in both positive and negative TWI and TPI areas, with a slight tendency for low-yield points to be in areas of high TWI for Limmared 12B.

In Tumba, according to Figure 13, within-field DEM ranges were: 73A (14.49 – 20.72 m) and 329A (41.1 – 60.01 m), indicating a stronger elevation gradient in 329A. Expected low-yield points appeared to be closer to a small stream located south of the field 329A compared to high-yield points. In addition, field 329A showed more of an undulating topography, compared to the rather flat field 73A.

For all fields, the TWI generated artefacts in the form of large areas of high TWI values. These artefacts were probably caused by low differences in elevation in most fields.

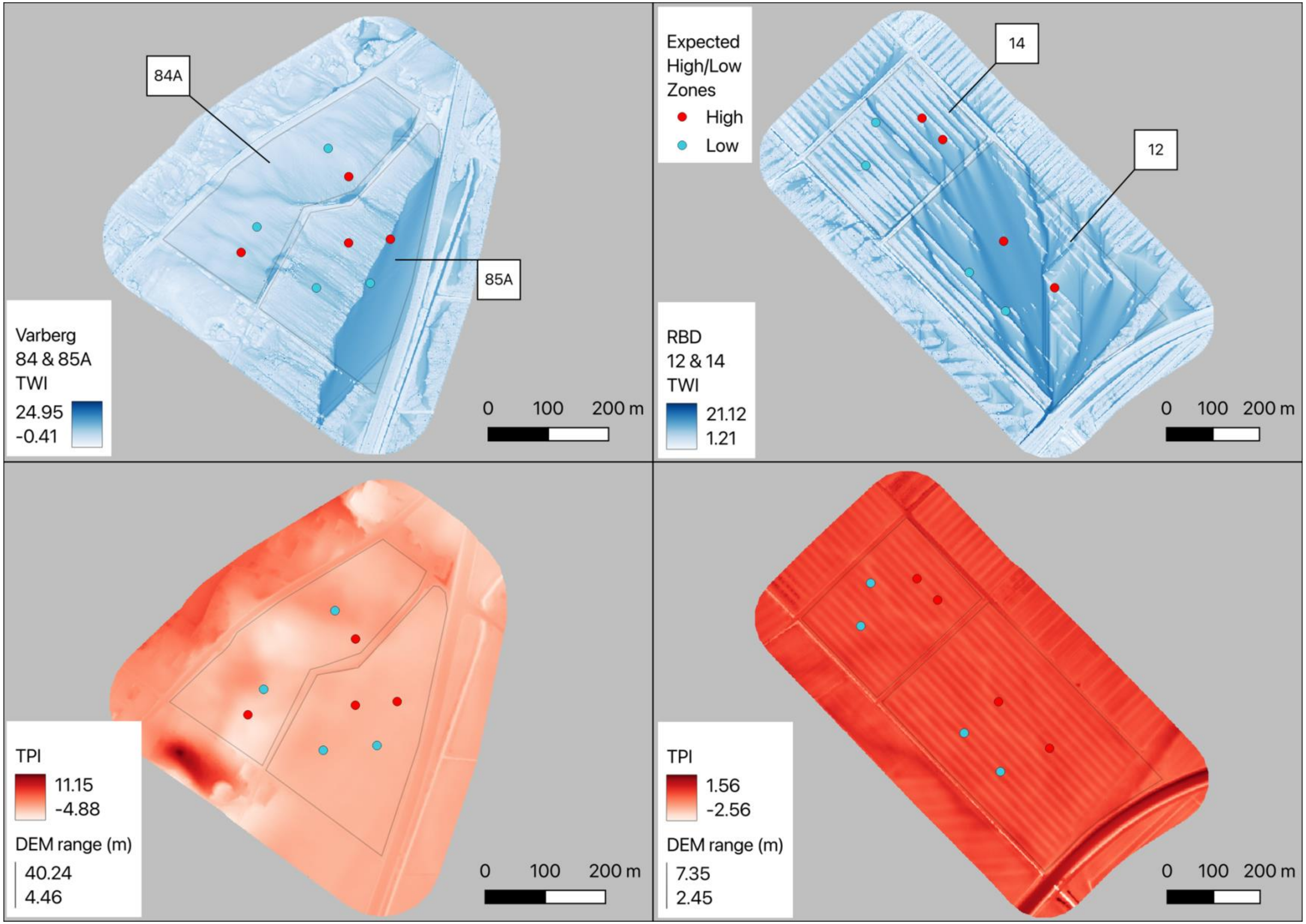

Figure 11: TWI and TPI for Varberg (left) and Röbäcksdalen (right). DEM ranges apply to visible buffers. Red and blue points apply to corresponding expected yield zones. Higher values indicate higher moisture for TWI and higher elevation for TPI.

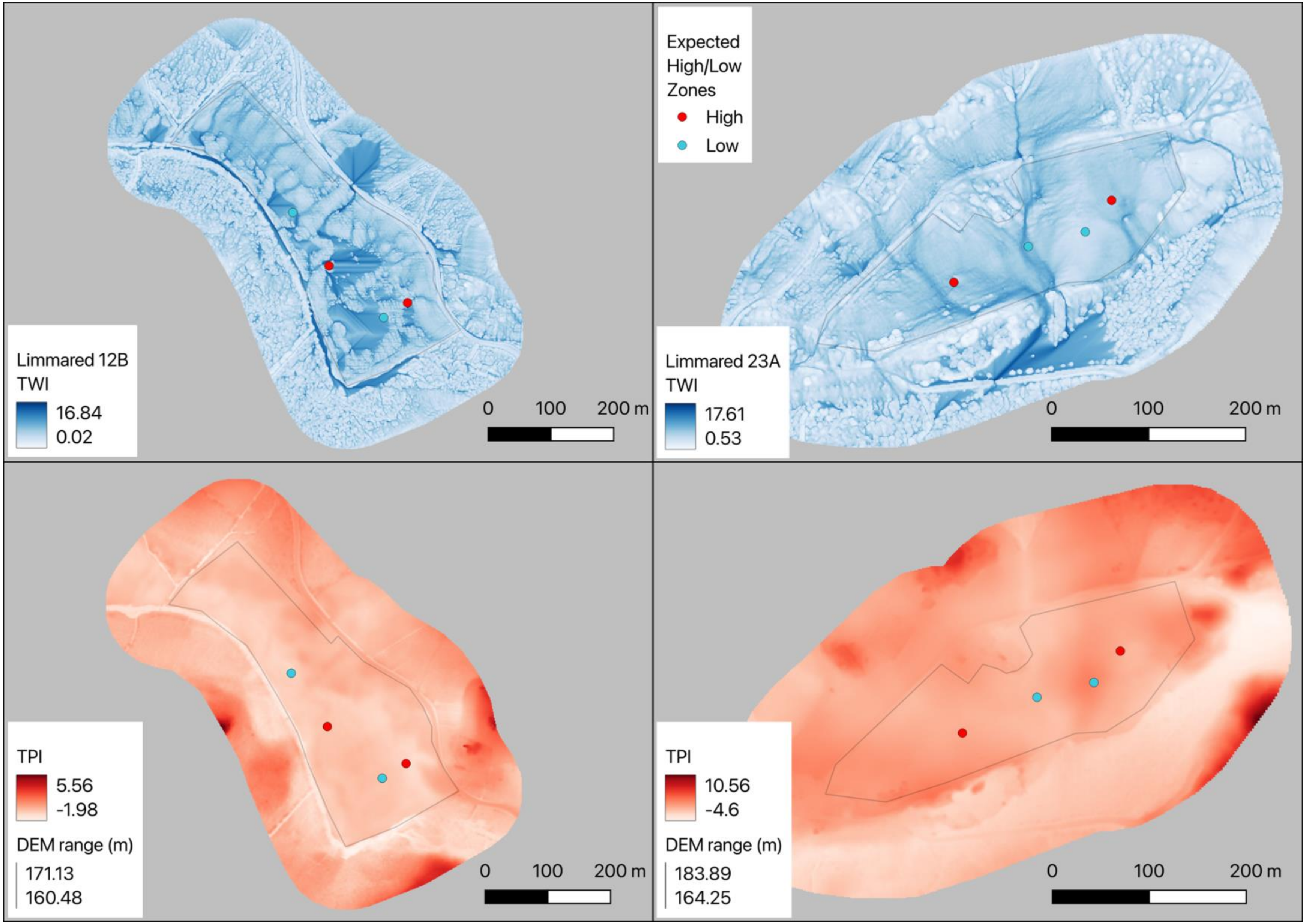

Figure 12: TWI and TPI for Limmared 12B (left) and Limmared 23A (right). DEM ranges apply for visible buffers. Red and blue points apply to corresponding expected yield zones. Higher values indicate higher moisture to TWI and higher elevation for TPI.

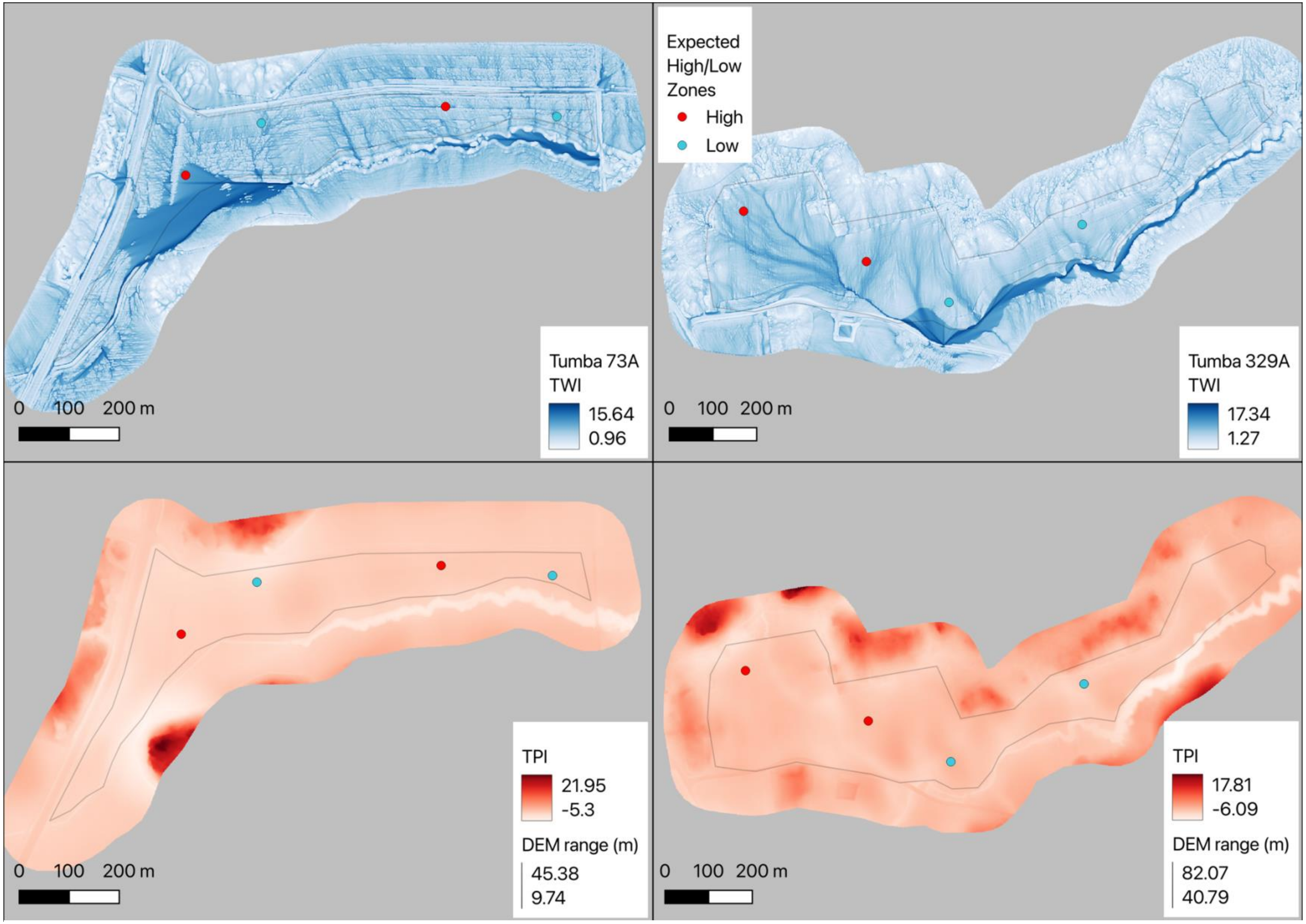

Figure 13: TWI and TPI for Tumba 73A (left) and Tumba 329A (right). DEM ranges apply to visible buffers. Red and blue points apply to corresponding expected yield zones. Higher values indicate higher moisture for TWI and higher elevation for TPI.

4. Discussion & Conclusion

4.1 Evaluation of Expected High- and Low-Yield Zones

Overall, the NDVI-based pre-selection of expected high- and low-yield zones was partly reflected in the field-based yield estimates. In most fields, the average estimated yield was higher in the expected high-yield zones than in the expected low-yield zones. This confirmation suggests that multi-year Sentinel-2 NDVI medians can capture some persistent spatial differences in ley productivity. However, the potential of this classification varied considerably across fields. The Sentinel-2-based yield classification was confirmed at Limmared 12B, where there was a clear difference between the estimated yields in high- and low-yield zones. The potential of the NDVI classification was limited or even reversed in fields such as Varberg 85A and Röbäcksdalen 14 (before the second harvest; Figure 3). In addition, before the third harvest, at Röbäcksdalen 14, the difference between expected high- and low- yield zones was negligibly small. This indicates that NDVI-based yield-zone classification can provide a useful starting point for identifying spatial productivity patterns, but it does not consistently predict field-measured biomass across all sites.

One possible explanation for this could be the fact that yield zones were defined using median NDVI time series during the ley growth seasons (2023 and 2024), whereas field sampling for this thesis was conducted on a single date in 2025 (two dates at Röbäcksdalen). The yield zone-classification, therefore, represents longer-term vegetation patterns rather than an exact biomass estimation for a sampling date. Also, weather patterns differed between the years of yield-zone selection (2023 & 2024) and the sampling year (2025). Most study sites received lower amounts of precipitation during the study period in 2025 when compared to the previous years. Temperature conditions were generally cooler in 2023 than in 2025 across all farms, whereas mean temperatures in 2024 were similar to 2025 for most study sites. Röbäcksdalen showed a clearer warming pattern, with 2025 being warmer than both previous years.

In addition, forage yields can vary considerably between growth cycles. Later growth cycles may be associated with higher biomass accumulation, where warmer temperatures, sufficient precipitation and longer or more favourable regrowth conditions promote plant growth (Perotti et al. 2021). As a result, the relative difference between expected high- and low-yield zones and the estimated yields in 2025 may change during the growing season. A zone initially classified as high-yield zone may not necessarily show higher biomass at an early sampling date but may still express higher productivity later in the season. This pattern may have been observed in Röbäcksdalen field 14 (Figure 3), where the expected high-yield zones (2551 kg ha^{-1}) showed a lower estimated yield than the low-yield zones (2718 kg ha^{-1}) before the second harvest, but a slightly higher estimated yield before the third harvest (3880 kg ha^{-1} in the high-yield zones and 3801 kg ha^{-1} in the low yield zones). Although this observation is based on a single field and the exact vegetation sampling points may have varied between the two sampling dates, it might suggest that growth-cycle effects and sampling timing could partly explain why the NDVI-based classification was not consistently reflected in the field-measured yields. However, this interpretation should be treated cautiously, as the estimated yield differences were small and may partly reflect random variation.

Another factor that may have led to irregular results may have been the scale of classification and vegetation sampling. Classification was based on Sentinel-2 pixels of approximately 10 x 10 m^2, whereas vegetation was collected from three smaller quadrats (0.25 m^2) within each pixel. If biomass varied substantially within a pixel, the quadrat samples may not have fully represented the satellite-derived yield-zone classification.

4.2 Explanatory Value of Satellite-Derived Spectral Indices

When evaluating all farms together, NDVI, EVI, NDRE (B5) and NDMI generally showed positive relationships with average estimated yield, whereas NDRE (B7), NDWI and BSI showed negative relationships (Figure 5).
The overall positive linear relationship between estimated yield and NDVI, EVI, NDRE (B5) and NDMI is physically plausible because these indices are, among others, related to canopy greenness, chlorophyll status, vegetation structure or vegetation water content (Gao 1996; Huete et al. 2002; Jones et al. 2007; Jiang et al. 2008). However, the relationship between vegetation indices and dry matter yield was not consistent across all sites. This highlights that spectral indices should be interpreted as indicators of canopy reflectance properties rather than direct measurements of harvested dry matter yield. Reflectance responses may be influenced by various factors such as greenness, vegetation structure, water content, chlorophyll status, botanical composition or growth stage, not only by dry biomass (Garroutte et al. 2016; Perotti et al. 2021).

NDVI showed a narrower response range than EVI (Figure 5), which may reflect its known tendency to saturate under dense or high-biomass vegetation conditions. EVI was developed to improve sensitivity in high-biomass regions and to reduce atmospheric and canopy-background effects compared with NDVI (Huete et al. 2002). The more responsive behaviour of EVI in this study, therefore, supports its usefulness for detecting canopy differences in densely vegetated ley fields, although EVI also did not consistently explain yield differences across all farms.

The positive relationship between NDMI and estimated yield may indicate that higher-yielding areas also had higher vegetation water content. This interpretation is consistent with the formulation of NDMI, which uses near-infrared and shortwave-infrared reflectance and is therefore sensitive to vegetation water-related properties (Gao 1996). In addition, Subhashree et al. (2025) included NDMI in a pasture biomass-yield prediction framework and found it to be among the important vegetation-index predictors. However, NDMI should not be interpreted as a direct biomass measure, but rather as a moisture-related spectral indicator that may be associated with biomass under certain site and growth conditions.

The negative relationship between NDWI and estimated yield (Figure 5) can be explained by the formulation of the NDWI, which contrasts green and near-infrared reflectance. Because dense, healthy vegetation typically reflects strongly in the near-infrared region, vegetated surfaces can produce low or negative NDWI values (McFeeters 1996). Consequently, areas with more developed vegetation and higher biomass may show lower NDWI values. The observed negative relationship between NDWI and yield should therefore be interpreted as a spectral response of dense vegetation.

The negative relationship observed for NDRE (B7; Figure 5) should not necessarily be interpreted as a direct physiological relationship in which higher yield reduces red-edge response. Instead, it may reflect the spectral behaviour of the specific band combination used. In contrast to NDRE (utilising S-2 B5, 705 nm), NDRE (utilising S-2 B7, 783 nm) combines two bands that are both located close to the near-infrared plateau. As a result, the index may be less sensitive to chlorophyll-related absorption differences and more influenced by canopy structure or site-specific reflectance conditions. This interpretation is supported by Clevers & Gitelson (2013), who found that red-edge indices for canopy chlorophyll and nitrogen estimation performed best when a near-infrared band around 800 nm was combined with a denominator band in the 700-720 nm range, corresponding more closely to Sentinel-2 B5 than to B7. Therefore, the stronger and more interpretable relationship of NDRE (B5), compared with the more dispersed or negative behaviour of NDRE (B7), may be related to the lower chlorophyll sensitivity of the B8A-B7 combination.

The negative relationship between BSI and estimated yield is also physically plausible because BSI enhances the spectral contrast between bare soil and vegetation. Bare or sparsely vegetated surfaces tend to show relatively high red and shortwave-infrared reflectance, whereas dense vegetation is characterised by strong near-infrared reflectance and red-light absorption by chlorophyll. Consequently, higher-yielding areas with denser vegetation cover would be expected to have lower BSI values, while lower-yielding or more vegetated areas would show higher BSI values. This is consistent with the use of BSI as an indicator of bare soil, which negatively correlates with NDVI (Mzid et al. 2021).

One possible explanation for cases with relatively low index values but high estimated yield could be that vegetation indices mainly capture canopy greenness, chlorophyll content and spectral canopy properties rather than biomass directly. Nitrogen dilution during high biomass accumulation, species-specific differences in chlorophyll content and canopy colour and saturation of standard NDVI in dense vegetation may have therefore weakened the relationships between vegetation indices and measured yields (Mutanga & Skidmore 2004; Reyes et al. 2015; Suter et al. 2026).

The use of more sophisticated analytical methods may also improve the robustness of yield estimation. For example, Peng et al. (2023) used Sentinel-2 imagery to estimate dry matter yield in harvested forage fields in northern Sweden and found that vegetation indices were useful, but that more complex modelling approaches were needed for robust yield estimation. These may include more advanced multivariate or machine-learning regression methods.

4.3 Soil, Topography and Meteorological Influences

Soil

The soil data suggest that soil heterogeneity may have contributed to yield variability, but mainly in a field-specific way rather than as a consistent explanatory factor across all study sites. This indicates that the expected high- and low-yield zones were not controlled by one dominant soil variable. Instead, several soil properties likely interacted, including texture, organic matter, pH and nutrient availability. This is consistent with the broader understanding that crop growth is affected by the combined influence of soil physical and chemical conditions (Habib-ur-Rahman et al. 2022).

A particularly important implication is that apparently favourable soil properties cannot be interpreted in isolation. For example, high humus content would generally be expected to support soil fertility and water retention (Piccolo 1996), but its potential positive effect may be limited where other chemical constraints occur, such as low pH or elevated aluminium availability (as can be seen in field 12B, Limmared; see Figure 8 and Figure 9). High aluminium levels combined with low pH can lead to acidity-related yield constraints, which in turn could partly explain the low yields in these areas (Moir & Moot 2010). The expected high-yield zone in Tumba 73A showed more favourable soil conditions, including higher pH, higher K-AL, Mg-AL, Ca-AL and K-HCl, lower Al-AL and a finer texture with more clay and silt. These parameters are agronomically relevant because soil pH affects nutrient availability and aluminium mobility, while K-AL, Mg-AL and Ca-AL indicate the supply of plant-available base cations. In Swedish soil testing, K-HCl is also used as an indicator of the long-term potassium-supplying capacity of the soil and clay content can contribute to larger potassium reserves. Therefore, the high-yield zone can be interpreted as having both a more favourable acidity/base-cation status and a stronger potassium reserve than the low zone (Brady & Weil 2016; Emelie Andersson et al. 2023). On the other hand, expected high-yield zones in Tumba 329A had less favourable values for the aforementioned parameters than the low-yield zones, while still having higher estimated yields. This supports the fact that soil properties alone cannot explain the yield variability observed in this study.

Furthermore, the observed differences in soil chemical properties may partly reflect differences in field history. For example, parts of the field may previously have differed in land use, soil type or management intensity before being merged into a single field. In Limmared 12B, such historical variation could be relevant, as parts of the field may formerly have consisted of peat soil that has since been mineralised, while peat remains only in some areas. This could contribute to spatial differences in soil organic matter and related chemical properties. In addition, nutrients such as phosphorus can accumulate in areas that historically received higher manure inputs, for example close to former barns. Because phosphorus is relatively immobile in soil, such legacy effects may remain detectable long after the original management practice has ended (Brady & Weil 2016).

Overall, the soil results support the interpretation that yield variability in the studied ley fields was multi-factorial. Soil properties provided useful context for explaining some solitary field-specific patterns, especially where strong contrasts in pH, aluminium, texture or nutrient status were present. However, they did not provide a general explanation for the high- and low-yield classification or estimated yields. Therefore, soil conditions should be interpreted as one possible driver of spatial yield variability, rather than as the sole explanation for the observed yield-zone differences.

Topography

The topographic analysis provided some insight into potential water redistribution within fields, but it did not offer a consistent explanation for the expected high- and low-yield zones or estimated yields. This suggests that terrain position alone was not the dominant driver of yield variability in the studied ley fields. Although TWI and TPI can theoretically indicate differences in moisture accumulation (Kopecký et al. 2021) and relative landscape position, which can influence biomass production (Weiss 2001; Macdonald et al. 2025) both expected high- and low-yield points occurred across a range of topographic conditions.

Nevertheless, topography may still have contributed to the yield variability in specific fields. The maps suggest that some fields had clearer micro-topographic structures than others, particularly Röbäcksdalen and Tumba 329A. In such cases, local depressions, drainage pathways or proximity to lower-lying areas may influence soil moisture availability and thereby positively affect vegetation development (Macdonald et al. 2025). However, the absence of a consistent relationship between yield zones and TWI/TPI indicates that these terrain-derived indices were not sufficient to explain yield variability on their own. In addition, TWI derives possible soil moisture only from topography. Other factors, such as soil texture, are not considered, which may in turn produce unrealistic results.

Another major limitation is that several fields were relatively flat, which reduced the reliability of the TWI. Flat agricultural landscapes with small elevation differences can strongly affect calculated flow accumulation and produce unrealistic TWI patterns (Schmidt & Persson 2003). This was visible in the occurrence of large areas with high TWI values (e.g. Figure 11), which likely represent artefacts rather than actual soil moisture conditions. Therefore, TWI in this thesis should be cautiously interpreted as an indicator of potential wetness. Direct soil moisture measurements or drainage information would be needed to confirm whether the mapped wetness patterns are actually realistic.

To conclude, the topographic results support the broader interpretation that yield variability was controlled by several interacting factors rather than by one single environmental gradient. TWI and TPI should be treated as contextual variables that may help interpret local patterns, rather than as robust predictors of high- and low-yield zones across the study sites.

Meteorology

Differences in precipitation and temperature before sampling may have contributed to variation in estimated yield between farms and sampling dates. This interpretation is supported by Perotti et al. (2021), who found that temperature and precipitation were among the main drivers of forage yield and quality in intensively managed grasslands and that the relative importance of these drivers differed between growth cycles. In the first growth cycle, yield was mainly associated with grass proportion, precipitation and temperature. During the second growth cycle, grass proportion and temperature were the most relevant yield-related factors, whereas in the third growth cycle, yield was primarily associated with soil nitrogen availability, precipitation and grass proportion.

Considering the average estimated yield per farm (Figure 3), Varberg showed the highest yield (2526.67 kg ha^{-1}) among the June sampling sites. This may be partly explained by the comparatively favourable pre-sampling conditions with higher observed precipitation than for Limmared or Tumba. In contrast, Tumba had the lowest average estimated yield (2040.67 kg ha^{-1}), which may be related to the particularly low precipitation recorded before sampling. Röbäcksdalen before the third harvest showed the highest overall estimated yield (3922.35 kg ha^{-1}). As discussed above, this is likely influenced by the later sampling date and different growth cycle, but the relatively favourable precipitation and temperature conditions before the third harvest may also have supported biomass accumulation. Therefore, differences in pre-sampling weather conditions may partly explain variation in estimated yield between farms and sampling dates.

4.4 Limitations

Limitations should be considered when interpreting the results of this thesis. First, the number of sampling points was limited, with only two expected high-yield and two expected low-yield pixels per field over one year. This limited the possibility of drawing strong statistical conclusions and suggests that individual sampling locations may have had a large influence on the observed field-level patterns. Second, the yield-zone classification was based on Sentinel-2 NDVI medians from 2023 and 2024, whereas field sampling was conducted in 2025.

Another limitation was the scale mismatch between satellite data and yield measurements. Sentinel-2 pixels represent an area of approximately 10 x 10 m, whereas vegetation samples were collected from smaller quadrats within each pixel. Small-scale biomass variability within a pixel may therefore not have been fully captured by either the satellite signal or the quadrat samples.

Finally, some potentially important explanatory factors were not fully available or directly measured in some fields. These include detailed management information, cutting history, fertilisation, drainage conditions or direct soil moisture measurements. The topographic wetness index was also affected by artefacts in flat fields and should therefore be interpreted only as a potential indicator of wetness. Overall, these limitations mean that the results should be interpreted as exploratory and field-specific rather than as a general model of ley yield variability.

4.5 Conclusion

This thesis showed that NDVI-based high- and low-yield zones were partly reflected in field-based dry matter yield estimates, but that the classification did not perform consistently across all fields. While several spectral indices, especially NDVI, EVI, NDRE (B5) and NDMI, showed plausible relationships with estimated yield, these relationships varied between farms and growth stages. This indicates that satellite-derived indices are useful indicators of vegetation condition, but not direct or universally reliable measures of harvested dry matter yield.

Soil properties, topography and meteorological conditions provided additional context for interpreting yield variability, but none of them explained the observed patterns on their own, suggesting that yield variability resulted from interactions between the analysed factors. The study therefore suggests that NDVI-based yield-zone classification can be a useful starting point for identifying productivity patterns in ley fields, but should be combined with repeated field measurements and environmental data to produce reliable results. In addition, more advanced multivariate or machine-learning regression methods could be a better option for measuring within-field biomass variability.

References

Alexandersson, H. (2003). *Korrektion av nederbörd enligt enkel klimatologisk metodik [Correction of precipitation using a simple climatological method]*. Swedish Meteorological and Hydrological Institute. https://www.smhi.se/publikationer-fran-smhi/sok-publikationer/2003-05-11-korrektion-av-nederbord-enligt-enkel-klimatologisk-metodik.

Beck, H.E., McVicar, T.R., Vergopolan, N., Berg, A., Lutsko, N.J., Dufour, A., Zeng, Z., Jiang, X., Van Dijk, A.I.J.M. & Miralles, D.G. (2023). High-resolution (1 km) Köppen-Geiger maps for 1901–2099 based on constrained CMIP6 projections. *Scientific Data*, 10 (1), 724. https://doi.org/10.1038/s41597-023-02549-6

Beehler, J., Fry, J., Negassa, W. & Kravchenko, A. (2017). Impact of cover crop on soil carbon accrual in topographically diverse terrain. *Journal of Soil and Water Conservation*, 72 (3), 272–279. https://doi.org/10.2489/jswc.72.3.272

Beven, K.J. & Kirkby, M.J. (1979). A physically based, variable contributing area model of basin hydrology / Un modèle à base physique de zone d'appel variable de l'hydrologie du bassin versant. *Hydrological Sciences Bulletin*, 24 (1), 43–69. https://doi.org/10.1080/02626667909491834

Blair, J., Nippert, J. & Briggs, J. (2014). Grassland Ecology. In: Monson, R.K. (ed.) *Ecology and the Environment*. Springer New York. 389–423. https://doi.org/10.1007/978-1-4614-7501-9_14

Böhner, J. & Selige, T. (2006). Spatial Prediction of Soil Attributes Using Terrain Analysis and Climate Regionalisation., 2006. https://api.semanticscholar.org/CorpusID:135094533

Brady, N.C. & Weil, R.R. (2016). *The nature and properties of soils*. Fifteenth edition, global edition. Pearson. (Pearson global edition)

Cameron, K.C., Di, H.J. & Moir, J.L. (2013). Nitrogen losses from the soil/plant system: a review. *Annals of Applied Biology*, 162 (2), 145–173. https://doi.org/10.1111/aab.12014

Clevers, J.G.P.W. & Gitelson, A.A. (2013). Remote estimation of crop and grass chlorophyll and nitrogen content using red-edge bands on Sentinel-2 and -3. *International Journal of Applied Earth Observation and Geoinformation*, 23, 344–351. https://doi.org/10.1016/j.jag.2012.10.008

Conant, R.T., Cerri, C.E.P., Osborne, B.B. & Paustian, K. (2017). Grassland management impacts on soil carbon stocks: a new synthesis. *Ecological Applications*, 27 (2), 662–668. https://doi.org/10.1002/eap.1473

Delegido, J., Verrelst, J., Alonso, L. & Moreno, J. (2011). Evaluation of Sentinel-2 Red-Edge Bands for Empirical Estimation of Green LAI and Chlorophyll Content. *Sensors*, 11 (7), 7063–7081. https://doi.org/10.3390/s110707063

Drinkwater, L.E., Wagoner, P. & Sarrantonio, M. (1998). Legume-based cropping systems have reduced carbon and nitrogen losses. *Nature*, 396 (6708), 262–265. https://doi.org/10.1038/24376

Emelie Andersson, Gunilla Frostgård, Emma Hjelm, Pernilla Kvarmo, Maria Stenberg, & Johan Malgeryd (2023). *Rekommendationer för gödsling och kalkning 2024 [Recommendations for Fertilisation and Liming 2024]*. (Jordbruksinformation 17 – 2023). Jordbruksverket. https://stsigillblobsprod.blob.core.windows.net/media/1hhomjit/jordbruksverkets-rekommendationer-fo-r-go-dsling-och-kalkning-2024.pdf [2026-04-29]

European Space Agency (2024). *Sentinel-2 – Documentation*. *ESA*. https://documentation.dataspace.copernicus.eu/Data/SentinelMissions/Sentinel2.html [2026-04-07]
European Space Agency (2025). *Sentinel-2 Mission Overview*. https://sentiwiki.copernicus.eu/web/s2-mission [2026-04-21]
European Union/ESA/Copernicus (2021). *Sentinel-2 MSI: MultiSpectral Instrument, Level-2A [Harmonized]*. *Google Earth Engine Data Catalog*. https://developers.google.com/earth-engine/datasets/catalog/COPERNICUS_S2_SR_HARMONIZED [2026-04-21]
Florinsky, I.V. (2016). Digital Elevation Models. In: *Digital Terrain Analysis in Soil Science and Geology*. Elsevier. 77–108. https://doi.org/10.1016/B978-0-12-804632-6.00003-1
Gao, B. (1996). NDWI—A normalized difference water index for remote sensing of vegetation liquid water from space. *Remote Sensing of Environment*, 58 (3), 257–266. https://doi.org/10.1016/S0034-4257(96)00067-3
Garroutte, E., Hansen, A. & Lawrence, R. (2016). Using NDVI and EVI to Map Spatiotemporal Variation in the Biomass and Quality of Forage for Migratory Elk in the Greater Yellowstone Ecosystem. *Remote Sensing*, 8 (5), 404. https://doi.org/10.3390/rs8050404
Gibson, D.J. (2009). *Grasses and grassland ecology*. First edition. Oxford University Press. (Oxford biology)
Gitelson, A.A., Gritz †, Y. & Merzlyak, M.N. (2003). Relationships between leaf chlorophyll content and spectral reflectance and algorithms for non-destructive chlorophyll assessment in higher plant leaves. *Journal of Plant Physiology*, 160 (3), 271–282. https://doi.org/10.1078/0176-1617-00887
Habib-ur-Rahman, M., Raza, A., Ahrends, H.E., Hüging, H. & Gaiser, T. (2022). Impact of in-field soil heterogeneity on biomass and yield of winter triticale in an intensively cropped hummocky landscape under temperate climate conditions. *Precision Agriculture*, 23 (3), 912–938. https://doi.org/10.1007/s11119-021-09868-x
Hayes, S., Cawkwell, F., Bacon, K.L. & Wingler, A. (2025). Remote Sensing of Grassland Plant Biodiversity and Functional Traits. *Ecology and Evolution*, 15 (8), e71829. https://doi.org/10.1002/ece3.71829
Hoeffner, K., Hotte, H., Cluzeau, D., Charrier, X., Gastal, F. & Pérès, G. (2021). Effects of temporary grassland introduction into annual crop rotations and nitrogen fertilisation on earthworm communities and forage production. *Applied Soil Ecology*, 162, 103893. https://doi.org/10.1016/j.apsoil.2021.103893
Horning, N. (2019). Remote Sensing. In: *Encyclopedia of Ecology*. Elsevier. 404–413. https://doi.org/10.1016/B978-0-12-409548-9.10607-4
Huete, A., Didan, K., Miura, T., Rodriguez, E.P., Gao, X. & Ferreira, L.G. (2002). Overview of the radiometric and biophysical performance of the MODIS vegetation indices. *Remote Sensing of Environment*, 83 (1–2), 195–213. https://doi.org/10.1016/S0034-4257(02)00096-2
Huss-Danell, K., Chaia, E. & Carlsson, G. (2007). N2 fixation and nitrogen allocation to above and below ground plant parts in red clover-grasslands. *Plant and Soil*, 299 (1–2), 215–226. https://doi.org/10.1007/s11104-007-9376-4
Jiang, Z., Huete, A., Didan, K. & Miura, T. (2008). Development of a two-band enhanced vegetation index without a blue band. *Remote Sensing of Environment*, 112 (10), 3833–3845. https://doi.org/10.1016/j.rse.2008.06.006

Johansson, B. (2000). Areal Precipitation and Temperature in the Swedish Mountains. *Hydrology Research*, 31 (3), 207–228. https://doi.org/10.2166/nh.2000.0013
Johansson, B. & Chen, D. (2003). The influence of wind and topography on precipitation distribution in Sweden: statistical analysis and modelling. *International Journal of Climatology*, 23 (12), 1523–1535. https://doi.org/10.1002/joc.951
Johansson, B. & Chen, D. (2005). Estimation of areal precipitation for runoff modelling using wind data: a case study in Sweden. *Climate Research*, 29, 53–61. https://doi.org/10.3354/cr029053
Johnson, F.E., Roth, R.T., Ruffatti, M.D. & Armstrong, S.D. (2024). Cover crop impacts on nitrogen losses and environmental damage cost. *Agriculture, Ecosystems & Environment*, 363, 108859. https://doi.org/10.1016/j.agee.2023.108859
Jones, C.L., P. R. Weckler, N. O. Maness, R. Jayasekara, M. L. Stone, & D. Chrz (2007). Remote Sensing to Estimate Chlorophyll Concentration in Spinach Using Multi-Spectral Plant Reflectance. *Transactions of the ASABE*, 50 (6), 2267–2273. https://doi.org/10.13031/2013.24079
Kopecký, M., Macek, M. & Wild, J. (2021). Topographic Wetness Index calculation guidelines based on measured soil moisture and plant species composition. *Science of The Total Environment*, 757, 143785. https://doi.org/10.1016/j.scitotenv.2020.143785
Kravchenko, A.N. & Bullock, D.G. (2000). Correlation of Corn and Soybean Grain Yield with Topography and Soil Properties. *Agronomy Journal*, 92 (1), 75–83. https://doi.org/10.2134/agronj2000.92175x
Kravchenko, A.N., Thelen, K.D., Bullock, D.G. & Miller, N.R. (2003). Relationship among Crop Grain Yield, Topography, and Soil Electrical Conductivity Studied with Cross-Correlograms. *Agronomy Journal*, 95 (5), 1132–1139. https://doi.org/10.2134/agronj2003.1132
Lantmäteriet (2026). *Markhöjdmodell [Digital Elevation Model; DEM]. Lantmateriet.se*. https://www.lantmateriet.se/sv/geodata/vara-produkter/produktlista/markhojdmodell-nedladdning [2026-04-13]
Li, S., Xu, L., Jing, Y., Yin, H., Li, X. & Guan, X. (2021). High-quality vegetation index product generation: A review of NDVI time series reconstruction techniques. *International Journal of Applied Earth Observation and Geoinformation*, 105, 102640. https://doi.org/10.1016/j.jag.2021.102640
Macdonald, J.A., Barnard, D.M., Mankin, K.R., Miner, G.L., Erskine, R.H., Poss, D.J., Mehan, S., Mahood, A.L. & Mikha, M.M. (2025). Topographic Position Index Predicts Within-Field Yield Variation in a Dryland Cereal Production System. *Agronomy*, 15 (6), 1304. https://doi.org/10.3390/agronomy15061304
McFeeters, S.K. (1996). The use of the Normalized Difference Water Index (NDWI) in the delineation of open water features. *International Journal of Remote Sensing*, 17 (7), 1425–1432. https://doi.org/10.1080/01431169608948714
Meurer, K.H.E., Bolinder, M.A., Andrén, O., Hansson, A.-C., Pettersson, R. & Kätterer, T. (2019). Shoot and root production in mixed grass ley under daily fertilization and irrigation: validating the N productivity concept under field conditions. *Nutrient Cycling in Agroecosystems*, 115 (1), 85–99. https://doi.org/10.1007/s10705-019-10006-3
Milazzo, F., Francksen, R.M., Zavattaro, L., Abdalla, M., Hejduk, S., Enri, S.R., Pittarello, M., Price, P.N., Schils, R.L.M., Smith, P. & Vanwalleghem, T. (2023). The role of grassland for erosion and flood mitigation in Europe:

A meta-analysis. *Agriculture, Ecosystems & Environment*, 348, 108443. https://doi.org/10.1016/j.agee.2023.108443
Moir, J.L. & Moot, D.J. (2010). Soil pH, exchangeable aluminium and lucerne yield responses to lime in a South Island high country soil. *Proceedings of the New Zealand Grassland Association*, 191–195. https://doi.org/10.33584/jnzg.2010.72.2788
Moore, I.D., Grayson, R.B. & Ladson, A.R. (1991). Digital terrain modelling: A review of hydrological, geomorphological, and biological applications. *Hydrological Processes*, 5 (1), 3–30. https://doi.org/10.1002/hyp.3360050103
Mutanga, O. & Skidmore, A.K. (2004). Narrow band vegetation indices overcome the saturation problem in biomass estimation. *International Journal of Remote Sensing*, 25 (19), 3999–4014. https://doi.org/10.1080/01431160310001654923
Mzid, N., Pignatti, S., Huang, W. & Casa, R. (2021). An Analysis of Bare Soil Occurrence in Arable Croplands for Remote Sensing Topsoil Applications. *Remote Sensing*, 13 (3), 474. https://doi.org/10.3390/rs13030474
Oenema, J., Noij, G.J., Vlugt, P. van der & Kempenaar, C. (2024). Does precision N-fertilizer application in grassland make sense? *Proceedings of 30th General Meeting of the European Grassland Federation (EGF2024): Why grasslands?*, 2024. 639–641. Brill. https://research.wur.nl/en/publications/does-precision-n-fertilizer-application-in-grassland-make-sense/ [2026-04-25]
Parsons, D., Nadeau, E., Sousa, D., Åkerfeldt, M., Bernes, G., Hansson, P., Åhman, B., Palmborg, C., Picasso, V., Micke, B., Knicky, M., Arvidsson Segerkvist, K., Bergqvist, S., Rustas, B.-O., Lidfeldt, M., Remvig, S. & Wallsten, J. (2024). *Leys from a Nordic perspective : a knowledge compilation*. Department of Crop Production Ecology, Swedish University of Agricultural Sciences. https://doi.org/10.54612/a.1kvv46i0hf
Peng, J., Morel, J., Oliveira, J. & Parsons, D. (2024). Ley field management using satellite based digital tools. *Proceedings of 30th European Grassland Federation General Meeting (EGF 2024): Why grasslands?*, Leeuwarden, The Netherlands, 2024. European Grassland Federation (EGF). https://res.slu.se/id/publ/131396
Peng, J., Zeiner, N., Parsons, D., Féret, J.-B., Söderström, M. & Morel, J. (2023). Forage Biomass Estimation Using Sentinel-2 Imagery at High Latitudes. *Remote Sensing*, 15 (9), 2350. https://doi.org/10.3390/rs15092350
Perotti, E., Huguenin-Elie, O., Meisser, M., Dubois, S., Probo, M. & Mariotte, P. (2021). Climatic, soil, and vegetation drivers of forage yield and quality differ across the first three growth cycles of intensively managed permanent grasslands. *European Journal of Agronomy*, 122, 126194. https://doi.org/10.1016/j.eja.2020.126194
Persson, T., Murguzur, F.J.A., Davids, C., Höglind, M. & Jørgensen, M. (2024). Combining satellite-sensed and ground data and the BASGRA model to predict grass yield in high-latitude regions. *Field Crops Research*, 318, 109610. https://doi.org/10.1016/j.fcr.2024.109610
Peyraud, J.-L. & Peeters, A. (2016). The role of grassland-based production system in the protein security. *Proceedings of 26th General Meeting of the European Grassland Federation*, Trondheim, Norway, September 2016. European Grassland Federation
Piccolo, A. (1996). Humus and Soil Conservation. In: *Humic Substances in Terrestrial Ecosystems*. Elsevier. 225–264. https://doi.org/10.1016/B978-044481516-3/50006-2

Pradham, P., Younan, N.H. & King, R.L. (2008). Concepts of image fusion in remote sensing applications. In: *Image Fusion*. Elsevier. 393–428. https://doi.org/10.1016/B978-0-12-372529-5.00019-6
Reinermann, S., Asam, S. & Kuenzer, C. (2020). Remote Sensing of Grassland Production and Management—A Review. *Remote Sensing*, 12 (12), 1949. https://doi.org/10.3390/rs12121949
Reyes, J., Schellberg, J., Siebert, S., Elsaesser, M., Adam, J. & Ewert, F. (2015). Improved estimation of nitrogen uptake in grasslands using the nitrogen dilution curve. *Agronomy for Sustainable Development*, 35 (4), 1561–1570. https://doi.org/10.1007/s13593-015-0321-2
Robert, P.C. (2002). Precision agriculture: a challenge for crop nutrition management. *Plant and Soil*, 247 (1), 143–149. https://doi.org/10.1023/A:1021171514148
Rouse, J.W.R., Haas, R.H., Schell, J.A. & Deering, D.W. (1973). Monitoring Vegetation Systems in the Great Plains with ERTS (Earth Resources Technology Satellite)., Greenbelt, Maryland, USA, December 10 1973. 309–317. NASA
Schmidt, F. & Persson, A. (2003). Comparison of DEM Data Capture and Topographic Wetness Indices. *Precision Agriculture*, 4 (2), 179–192. https://doi.org/10.1023/A:1024509322709
Shi, A., Nunan, N., Figueira, J., Herrmann, A.M. & Wetterlind, J. (2022). Long-term ley and manure managements have consistent effects on microbial functional profiles and organic C groups across soils from a latitudinal gradient. *Agronomy for Sustainable Development*, 42 (6), 107. https://doi.org/10.1007/s13593-022-00837-w
SMHI (2024). *Dataserier med normalvärden för perioden 1991-2020 [Temperature series with normal values 1991–2020]*. *SMHI*. [text]. https://www.smhi.se/data/temperatur-och-vind/temperatur/dataserier-med-normalvarden-for-perioden-1991-2020 [2026-04-10]
SMHI (2025). *Griddad nederbörd- och temperaturdata [Gridded precipitation and temperature data]*. *SMHI*. [text]. https://www.smhi.se/data/nederbord-och-fuktighet/nederbord/griddad-nederbord--och-temperaturdata [2026-04-13]
Souza, E.G.D., Khosla, R., Sudduth, K.A., Johann, J.A. & Bazzi, C.L. (2025). Spatial and Temporal Variability in Yield Maps Can Localize Field Management—A Case Study with Corn and Soybean. *Agronomy*, 15 (5), 1179. https://doi.org/10.3390/agronomy15051179
Subhashree, S.N., Igathinathane, C., Hendrickson, J., Archer, D., Liebig, M., Halvorson, J., Kronberg, S., Toledo, D. & Sedivec, K. (2025). Evaluating Remote Sensing Resolutions and Machine Learning Methods for Biomass Yield Prediction in Northern Great Plains Pastures. *Agriculture*, 15 (5), 505. https://doi.org/10.3390/agriculture15050505
Suter, S., Welden, N., Roberts, K. & Barrett, B. (2026). Predicting species diversity and community traits from remote sensing in species-rich grasslands. *BMC Ecology and Evolution*, 26 (1), 21. https://doi.org/10.1186/s12862-026-02500-4
Suttie, J.M., Reynolds, S.G., & FAO (eds) (2005). *Grasslands of the world*. Food and Agriculture Organization of the United Nation. (FAO plant production and protection series; 34)
Tucker, C.J. (1979). Red and photographic infrared linear combinations for monitoring vegetation. *Remote Sensing of Environment*, 8 (2), 127–150. https://doi.org/10.1016/0034-4257(79)90013-0
Van Der Meer, F., Bakker, W., Scholte, K., Skidmore, A., De Jong, S., Clevers, J., Addink, E. & Epema, G. (2001). Spatial scale variations in vegetation indices and above-ground biomass estimates: Implications for MERIS.

International Journal of Remote Sensing, 22 (17), 3381–3396. https://doi.org/10.1080/01431160152609227

Van ’T Hull, J., Van Middelkoop, J., Van Schooten, H., Ros, M., Van Groenigen, J.W. & Velthof, G. (2025). Potential measures to reduce nitrate and nitrous oxide losses from renovated grasslands. *Agriculture, Ecosystems & Environment*, 384, 109549. https://doi.org/10.1016/j.agee.2025.109549

Vélez, S., Martínez-Peña, R. & Castrillo, D. (2023). Beyond Vegetation: A Review Unveiling Additional Insights into Agriculture and Forestry through the Application of Vegetation Indices. *J*, 6 (3), 421–436. https://doi.org/10.3390/j6030028

Vitousek, P.M. (2015). Grassland ecology: Complexity of nutrient constraints. *Nature Plants*, 1 (7), 15098. https://doi.org/10.1038/nplants.2015.98

Wang, L. & Liu, H. (2006). An efficient method for identifying and filling surface depressions in digital elevation models for hydrologic analysis and modelling. *International Journal of Geographical Information Science*, 20 (2), 193–213. https://doi.org/10.1080/13658810500433453

Weiss, A. (2001). Topographic Position and Landforms Analysis. Poster presentation. https://www.jennessent.com/downloads/TPI-poster-TNC_18x22.pdf [2026-04-25]

White, R.P., Murray, S., Rohweder, M. & Prince, S.D. (2000). *Pilot analysis of global ecosystems: grassland ecosystems*. World Resources Institute. (PAGE: Pilot analysis of global ecosystems)

Zevenbergen, L.W. & Thorne, C.R. (1987). Quantitative analysis of land surface topography. *Earth Surface Processes and Landforms*, 12 (1), 47–56. https://doi.org/10.1002/esp.3290120107

Zhang, J. & Li, J. (2023). Spacecraft. In: *Spatial Cognitive Engine Technology*. Elsevier. 129–162. https://doi.org/10.1016/B978-0-323-95107-4.00004-4

Popular Science Summary

Ley fields are grasslands that are grown for animal feed and are an important part of Swedish agriculture. However, these fields are not always equally productive across their whole area. Some parts of a field may produce more forage, while others produce less. Understanding these differences can help farmers use fertiliser more efficiently and manage their fields in a more sustainable way.

This thesis studied spatial yield variability in Swedish ley fields at four different locations, namely Varberg, Limmared, Tumba and Röbäcksdalen. The study compared field-based yield estimates (that means, the dry weight of vegetation samples from various parts of a field) with satellite data from the Sentinel-2 mission, soil properties, weather data and terrain information. Satellite data is often expressed with the help of spectral indices. Spectral indices, such as the Normalized Difference Vegetation Index (NDVI), the Enhanced Vegetation Index (EVI) or the Normalized Difference Moisture Index (NDMI), are mathematical combinations of satellite data that can be used to assess environmental conditions such as plant health and water availability. Before field sampling, so called high- and low-yield zones had been selected using satellite-based (NDVI) values from previous years. These zones were then compared with measured yields from vegetation samples collected in 2025.

The results showed that the selection of high- and low-yield zones using satellite data worked in many cases. Expected high-yield zones often had higher measured yields than expected low-yield zones. However, this potential was limited. In some cases, the difference was small or even reversed. Spectral indices such as NDVI, EVI, or NDMI were useful for describing plant conditions, but they did not always directly match the measured yield. Soil conditions, topography and weather helped explain some local patterns, but no single factor explained yield differences across all sites.

Overall, the study shows that satellite data can be a useful starting point for identifying productivity patterns in ley fields. However, reliable interpretation requires combining satellite information with field measurements and environmental data.

Publishing and archiving

Approved students' theses at SLU can be published online. As a student you own the copyright to your work and in such cases, you need to approve the publication. In connection with your approval of publication, SLU will process your personal data (name) to make the work searchable on the internet. You can revoke your consent at any time by contacting the library.

Even if you choose not to publish the work or if you revoke your approval, the thesis will be archived digitally according to archive legislation.

You will find links to SLU's publication agreement and SLU's processing of personal data and your rights on this page:

https://libanswers.slu.se/en/faq/228318

☒ YES, I, Wieland Schweizer, have read and agree to the agreement for publication and the personal data processing that takes place in connection with this.

☐ NO, I/we do not give my/our permission to publish the full text of this work. However, the work will be uploaded for archiving and the metadata and summary will be visible and searchable.